DOE/ET/23039-4
(DE82007333)

SYNTHESIS, EVALUATION AND DEFECT COMPENSATION OF TETRAHEDRAL GLASSES AS POSSIBLE SOLAR CELL MATERIALS

Final Report for the Period February 1, 1979—April 30, 1980

By
R. D. Rauh
T. L. Rose
A. N. Scoville

April 1980

Work Performed Under Contract No. AC03-79ET23039

EIC Corporation
Newton, Massachusetts

U.S. Department of Energy

Solar Energy

DISCLAIMER

DISCLAIMER

This report has been reproduced directly from the best available copy.

Available from the National Technical Information Service, U. S. Department of Commerce, Springfield, Virginia 22161.

Price: Printed Copy A03
Microfiche A01

Codes are used for pricing all publications. The code is determined by the number of pages in the publication. Information pertaining to the pricing codes can be found in the current issues of the following publications, which are generally available in most libraries: *Energy Research Abstracts, (ERA); Government Reports Announcements* and Index (*GRA* and I); *Scientific and Technical Abstract Reports (STAR);* and publication, NTIS-PR-360 available from (NTIS) at the above address.

DOE/ET/23039--4

DE82 007333

DOE/ET/23039-4
(DE82007333)
Distribution Category UC-63e

SYNTHESIS, EVALUATION AND DEFECT COMPENSATION OF TETRAHEDRAL GLASSES AS POSSIBLE SOLAR CELL MATERIALS

FINAL REPORT

February 1, 1979 - April 30, 1980

R. D. Rauh, Principal Investigator
T. L. Rose, Program Manager
A. N. Scoville, Staff Scientist

EIC Corporation, 55 Chapel Street
Newton, Massachusetts 02158

April, 1980

Sponsored by DOE Division of Solar Energy
Photovoltaics Program Office
UNDER CONTRACT NO. DE-AC03-79ET23039

ABSTRACT

The work at EIC Corporation during the first year of this contract was directed towards evaluation of new amorphous compounds for application in solar cells. The ternary $A^{II}B^{IV}C_2^V$ chalcopyrite systems were selected because of their inexpensive constituent elements and tetrahedral geometry. Polycrystalline samples of the ternary arsenides with Cd and Zn as the group II element and Ge, Si, Sn as the group IV element were synthesized. Attempts to prepare the analogous phosphide compounds were unsuccessful. Thin films were deposited by vacuum evaporation of the bulk ternary arsenides. The stoichiometries of the films were irreproducible and were usually deficient in the lower vapor pressure group IV element.

Films made by evaporating polycrystalline $ZnAs_2$, which also has a tetrahedral bonding structure, had stoichiometries generally in the range from Zn_3As_2 to $ZnAs_2$. The former compound is formed by the decomposition of $ZnAs_2$ to Zn_3As_2 and As_4. The intermediate stoichiometries are thought to be mixtures of the decomposition products. Preliminary results from annealing of the films indicate that heat treatment produces the stoichiometries expected for one of the two forms of zinc arsenide. The as-deposited films are amorphous when the substrate temperature is kept below 100°C.

The final half of the contract period was spent characterizing the a-$ZnAs_x$ films. EDAX and Auger analysis showed that films were homogeneous in the plane of the substrate, but that some variation occurred in the depth profile of the films. This change in composition is consistent with the sample decomposition which occurs during the evaporation. The as-prepared films were p-type with room temperature resistivities on the order of 10^2-$10^4\Omega$-cm. Optical absorption measurements gave optical band gap values of 1.2 eV for a-Zn_3As_2 and 1.5 eV for a-$ZnAs_2$. The $ZnAs_x$ films were photoconductive when irradiated with light of energy above the band gap.

The results on a-$ZnAs_x$ films have demonstrated that they possess three of the critical technical properties for application in solar cells: favorable band gap, strong absorption of the AM1 spectrum, and photoconductivity. They can also be formed by standard thin film techniques and are made from inexpensive and abundant materials. Further work will be directed towards doping the films and forming rectifying junctions to assess the photovoltaic properties of the material.

TABLE OF CONTENTS

LIST OF FIGURES

LIST OF TABLES

I. INTRODUCTION

Use of amorphous materials for solar cells offers a potentially simple and inexpensive method for fabrication of large solar cells. The research program described in this report was initially directed towards synthesis and evaluation of amorphous materials made up of ternary systems with the general formula $A^{II}B^{IV}C_2^V$ where A was Cd or Zn and C was P or As. Si, Ge, and Sn were selected as the group IV elements. These compounds were attractive for the following reasons:

- They are the structural analogs of $A^{III}B^V$ compounds with rigid tetrahedral bonding which should restrict dopants to fourfold coordination, allowing them to act as donors or acceptors.

- The class is so varied that changes in the ratio of the constituent elements permits adjustment of the band gap for maximum efficiency under solar irradiation using the most economical elements.

- The compounds have demonstrated a strong tendency towards glass formation.

- The materials are inexpensive and plentiful.

As the program developed, the large number of possible compounds was narrowed to Zn_3As_2 and $ZnAs_2$ which could be made as near stoichiometric films by evaporation of crystalline $ZnAs_2$. The elimination of the group IV element considerably simplified fabrication of the films. Virtually nothing was known about amorphous $ZnAs_2$ and very little about a-Zn_3As_2. The crystal forms, however, are well-characterized. $ZnAs_2$ is particularly interesting since it has the tetrahedrally coordinated bonding structure like the ternary systems, and analogous III-V compounds. The last half of the contract period was spent characterizing the zinc arsenide films.

The next section is a literature survey on the ternary compounds of Cd and Zn with P and As and the binary zinc arsenides. The physical, electrical and optical properties of the ternaries with Sn, Ge, or Si as the group IV element has been reported for the crystalline state, but the information is much less complete for the amorphous form. Section III presents a simple analysis of the defect structure in the ternary compounds. Understanding of the defect structure is essential for development of the methods for their compensation. The next two sections deal with preparations of bulk quantities of the ternary compounds and attempts to make stoichiometric films from them by vacuum evaporation. The poor results

obtained with the ternary compounds led to experiments with c-$ZnAs_2$ which is commercially available. Much better films were prepared with this compound. Section VI describes the results obtained in characterizing the chemical, physical, electrical and optical properties of the a-$ZnAs_x$ films. The final section contains an assessment of the $ZnAs_x$ films as a photovolatic material and recommends that additional work be done on this promising material.

II. LITERATURE SURVEY

A. $A^{II}B^{IV}C_2^V$ Tetrahedral Compounds

There is a good deal of information about the physical, electrical, and optical properties of the ternary $A^{II}B^{IV}C_2^V$ compounds in the crystalline state. Shay and Wernick have reviewed the literature prior to 1974 (1). A more recent review was published by Prochukhan and Rud (2). Table 1 lists the Zn and Cd compounds of interest in order of decreasing optical band gaps of the crystal. Also included are the reported ranges of resistivities and carrier concentrations at 300°K.

In the last three years, several laboratories have begun work on developing crystalline $A^{II}B^{IV}C_2^V$ systems for photovoltaic application. At the Research Triangle Institute, Dr. Andrews is working on the $ZnSiAs_2$ system (3) which grew out of earlier studies on $A^{II}B^{IV}C_2^V$ materials by Littlejohn et al. (4). Burton and Slack at Virginia Polytechnic Institute and State University are developing $CdSiAs_2$ thin film solar cells (5). Finally, a new program is underway at Exxon dealing with $ZnSnP_2$ as the crystalline chalcopyrite compound (6). Other papers of interest on the properties of $A^{II}B^{IV}C_2^V$ crystals include the papers of Brudnyi et al. (7) on the effect of electron irradiation on the electrical and optical properties of $ZnGeP_2$, $CdGeAs_2$, and $ZnSnAs_2$. Recent work appearing on the much-studied $CdGeAs_2$ system includes new features of the Cd-Ge-As phase diagram (8), and electrical and optical properties of large grain ingots (9). The following subjects were reported for the Zn ternary compounds: Ge doping of $ZnSiP_2$ (10), preparation of $ZnSiP_2$ (11) and $ZnGeP_2$ (12), and optical properties of $ZnGeP_2$ and $ZnGeAs_2$ (13).

The literature on the amorphous $A^{II}B^{IV}C_2^V$ compounds is much less extensive than for the crystalline state. There are short sections in Shay and Wernick's book (1) and in other reviews on semiconducting $A^{II}B^{IV}C_2^V$ compounds (14-16). We have carried out a computer search for all references since 1971 on amorphous Zn and Cd ternary chalcopyrites. Most of the work was done in Russia prior to 1972. Table 2 lists the available information on formation of the glassy compounds. The glasses are formed by rapid quenching of the melt, explosion in vacuum, or sputtering of the polycrystalline material. There are literature references for glass formation for all the materials except $ZnSiAs_2$, $ZnSnP_2$ and $CdSnP_2$. It is not known whether the absence of literature references is due to difficulty in preparation of the amorphous form or merely indicates that no attempts have been made. The tetragonal distortion for the three compounds is very small (1), and may make it difficult to form glasses by cooling of the melt. Uhlmann (17) has presented a model for evaluating the ease of glass formation, but it requires information that is not available for the compounds of interest.

TABLE 1

PROPERTIES OF TERNARY CHALCOPYRITE CRYSTALS (Ref. 2)

Compound	E_g^{min}(cry,eV)	Type	ρ(ohm cm)	n(cm^{-3})
$ZnSiP_2$	2.07	n	1.4×10^5	10^{13}-10^{18}
		p	10^9	10^{14}
$CdSiP_2$	2.05	n	10^2-10^7	10^{10}-10^{15}
		p	not observed	
$ZnGeP_2$	1.99	n	10^4	10^{13}-10^{15}
		p	10^2-10^8	10^{10}-10^{17}
$ZnSiAs_2$	1.74	n	10^9	10^8
		p	3.5×10^3	10^{13}-10^{17}
$CdGeP_2$	1.72	n	10^2-2×10^5	10^{11}-10^{14}
		p	4×10^3-10^8	10^{10}-4×10^{13}
$ZnSnP_2$	1.66	n	not observed	
		p	2-10	5×10^{16}-2×10^{17}
$CdSiAs_2$	1.55	n	1	10^{17}
		p	10^{-2}-10^3	10^{14}-10^{17}
$CdSnP_2$	1.16	n	10^{-3}-10^5	10^{15}-10^{18}
		p	10^3-10^4	10^{14}
$ZnCoAs_2$	1.15	n	not observed	
		p	10^{-1}-10^{-2}	4×10^{18}-10^{19}
$ZnSnAs_2$	0.73	n	10^2	10^{15}
		p	10^{-1}-10^{-4}	10^{17}-10^{21}
$CdGeAs_2$	0.57	n	10^{-1}-10^{-3}	10^{17}-10^{18}
		p	10^{-1}-10^2	10^{16}-10^{18}
$CdSnAs_2$	0.27	n	10^{-2}-10^{-4}	10^{17}-10^{18}
		p	1-50 $\times 10^{-2}$	10^{17}-6×10^{18}

TABLE 2

PROPERTIES OF $A^{II}B^{IV}C_2^V$ GLASSES

Compound	m.p. crystal (°C) (Ref. 1)	T_r(°C)[a]	E_g, glass (eV)[b]	Prep.[c]	Ref.
$ZnSiP_2$	1370,1250			f	d
$CdSiP_2$	1120		1.1(e)	g	16
$ZnGeP_2$	1027		1.1(e)	q	16
$ZnSiAs_2$	1096[d]	No information on glass formation			
$CdGeP_2$	778,795	485	1.1(o), 0.9(e)	q,e	e,f
$ZnSnP_2$	930	No information on glass formation			
$CdSiAs_2$	850,715	455	1.05(o), 1.4(e)	q	1
$CdSnP_2$	570	No information on glass formation			
$ZnGeAs_2$	850,875			e,s	f,g
$ZnSnAs_2$	775			f	16
$CdGeAs_2$	667,645	440	0.73(e), 0.53(o)	q,e	e,f
$CdSnAs_2$	595		0.15(e)	q	16

a - T_r = Recrystallization temperature

b - Band gap from (o) optical or (e) electrical measurements

c - Method of preparation:
- f = formed as film, conditions not specified
- q = glass made by rapid quenching of melt
- e = explosion in vacuum; film not same stoichiometry as bulk source
- s = sputtered film

d - P. Kirsten, V. Kulihauskus, K. S. Shishkin, Tr. Vses Soveshch. Fiz. Vzaimodeistviya Zaryazhennykh Chastits Monokist., 6th (1975), p. 433; CA 87, 172949v.

e - N. A. Goryunova, G. S. Kuzmenko and E. O. Osmanov, Nat. Sci. Eng., 7, 54 (1971).

f - V. G. Baryshev, N. S. Boltivets, A. S. Borshchevskii, N. A. Goryunova and P. T. Oreshkin, Sov. Phys. Semi., 4, 308 (1970).

g - W. Braun and M. Cardona, Phys. Stat. Sol. B, 76, 251 (1976).

The band gaps observed in the amorphous materials (see Table 2) do not form any systematic relationship when compared with the band gaps for the crystals. Moreover, there is little agreement between the band gap measured by electric measurement and the optical value. An interesting relationship has been proposed relating the recrystallization temperature to the band gap for materials of similar coordination number (18,19). For the limited data on the Cd ternaries, the relationship seems to hold. It will be of value, therefore, to determine the recrystallation temperature for the other amorphous materials not only to prevent recrystallization during annealing and formation of glasses but also to indicate the band gap of the material.

The vast majority of the work on amorphous $A^{II}B^{IV}C_2^V$ materials has been done on $CdGe_xM_{1-x}As_2$ where M is a group III, IV, or V metal atom and x ranges from 1 to 0. The simple ternary, x = 1, is the only $A^{II}B^{IV}C_2^V$ glass for which any electrical properties have been reported (20-23). Generally, the samples were n-type with resistances of $\simeq 1 \times 10^6$ ohm-cm at room temperature. The Seebeck coefficient became positive at reduced temperature and was a strong function of the fraction of Ge in the sample. The range of values obtained indicates the sensitivity of the material to the preparation conditions and impurity levels.

Recent work by Uemura on the four-element system with M = Si, Sn, and Pb and x = 1, 0.9 and 0.8 has shown ready glass formation with quenching of the melt (23). A study with M = Sb has also been reported (24). The results indicate that substitution of Pb and Sb reduce the band gap of the material. Si and Sn substitution, however, have much less effect on the amorphous material. These results are consistent with the substantial electrical and optical effects on CdM_xAs_2 glasses when M = Tl or Sb up to x = 0.8 (20).

Early reports of magnetic susceptibility measurements on amorphous CdM_xAs_2, where M = Ge, Si, Tl, Sb, indicated that there were paramagnetic centers in concentrations as high as $4 \times 10^{19} cm^{-3}$ (20,25). Later measurements, however, have shown that the levels must be less than $10^{17} cm^{-3}$ in $CdGeAs_2$ (26). Uemura's results also show no temperature dependence of the magnetic susceptibility indicating that paramagnetic centers are not introduced by substitution of up to 0.2 mole fraction of Si or Sn in place of Ge (23a). Modeling of the structure of glassy $CdGeAs_2$ is also consistent with a lack of homonuclear "wrong bonds" in the compound (27).

B. Zinc Arsenide

During the course of this work, it became apparent that the binary compounds found from zinc and arsenic might be suitable photovoltaic materials. Considerable work is being done on the analogous Zn_3P_2 system (6,28). Zinc arsenide forms crystal structures with two stoichiometries, Zn_3As_2 and $ZnAs_2$. The properties of the crystalline materials so far as they are known are given in Table 3. Although in amorphous materials the

TABLE 3[a]

PROPERTIES OF CRYSTALLINE Zn_3As_2 AND $ZnAs_2$

	Zn_3As_2	$ZnAs_2$
Phase	α (300 K) tetragonal, body centered α' (457 K) tetragonal, primitive β (945 K) cubic, face centered	monoclinic, primitive
m.p. (K)	1288	1041
Density ($g\text{-}cm^{-3}$)	5.6-5.7	5.0-5.12
$\Delta H_{f,298}$ (kcal/mole)	-33.7	-20.9
S°_{298} (eu/mole)	47.0	21.7
$\Delta H_{diss,298^{\circ}}$ (kcal/mole)	146.6	20.8
Resistivity (Ω-cm)	0.2(298 K)	$\parallel, 10^5$(77 K) $\perp, 10^2$(77 K)
Type	p	p
Hole Conc. (cm^{-3})	7×10^{17}	10^{16}
μ_H ($cm^2/V\text{-}sec$)	17	50
$\Delta E_{opt.}$ (eV)	0.93-1.0	0.92
Refractive Index[b]	3.85 ($\lambda > 4$ μm) 4.6_{max} ($\lambda = 1.1$ μm)	- -

[a] W. Zdanowicz and L. Zdanowicz, Annual Review of Materials Science, 5, 301 (1975).

[b] Ref. 31.

bonding is irregular compared to the crystal structure, the short range order in amorphous materials often reflects that of the crystalline material. For the Zn_3As_2 form, the Zn atom is four-coordinated with As atoms at the corners of a distorted tetrahedron while the As atom is six-coordinated with the Zn at six of the eight corners of a distorted cube. For $ZnAs_2$, on the other hand, the As is coordinated tetrahedrally to two Zn and two As atoms, while the Zn bonds to four As atoms (29). This bonding structure, particularly for the $ZnAs_2$ compound, results in a much more rigid structure than for materials such as the chalcogenides or amorphous As. The binary material structure is closer to that formed by the tetrahedrally coordinated group IV elements. Thus dopants might be restricted to fourfold coordination allowing them to act as donors or acceptors as in a-Si:H. The tetrahedral coordination is in contrast to the $CdAs_2$ isoelectronic material in which the As is only twofold coordinated presumably because the increased size of Cd compared to Zn leads to a larger separation between the As atoms. Thus, whereas for $CdAs_2$ addition to a group IV element is necessary to produce the rigid tetrahedral $CdM^{IV}As_2$ compound, this addition element is not necessary for the Zn containing arsenide.

The thermodynamically stable compound is the Zn_3As_2 species. Numerous studies have been done on the solid phase decomposition according to the reaction (30)

$$3ZnAs_2 \rightarrow Zn_3As_2 + As_4$$

This decomposition process leads to problems both in the synthesis of bulk $ZnAs_2$ crystals and the thermal evaporation of thin films of the material. Indeed this is the reason that most of the reported work has been done on the Zn_3As_2 species. In amorphous materials, however, the stoichiometric purity is less well-defined and some of the crystal properties, such as the band gap, are not appreciably different for the two compounds. One can expect, therefore, that the properties might be intermediate between the two forms in proportion to the stoichiometry of the amorphous material.

There is no information in the literature on the properties of a-$ZnAs_2$. Amorphous Zn_3As_2 thin films have been prepared by vacuum evaporation on glass substrates at 20°C (31). X-ray and electron diffraction showed no crystalline structure. The optical gap for the amorphous material was reported as 1.14 eV, about 0.2 eV larger than either the polycrystalline films formed at a substrate temperature of 200°C or the bulk crystalline material. The EO4 (energy at which the optical absorption is 10^4 cm^{-1}) reported was 1.28 eV. The films had a high refractive index which ranged from 4 to 4.6 in the region of maximum solar insolation indicating that an antireflective coating would be necessary for use of the material in a solar cell.

III. BONDING DEFECTS IN $A^{II}B^{IV}C_2^V$ GLASSES

Bonding defects in semiconducting materials can be generally categorized into those forming radical species and those leading to ionic defects (32). The first type arise from the dangling bonds as in α-Si whereas the latter have been proposed in the chalcogenides and $A^{III}B^V$ systems (33). Analyses of the $A^{II}B^{IV}C_2^V$ glasses of interest in this research shows that both types of defects are possible.

The structure for the simple $A^{II}C_2^V$ compounds is shown in Figure 1 using $CdAs_2$ as the example. The top picture gives a perspective view of the atom locations while the bottom is a schematic representation of the bonding around the tetrahedrally coordinated A^{II} atom. Two of the bonds to Cd are covalent and two are coordinate covalent (dative). Each arsenic forms a covalent bond, donates a pair of electrons for the dative bond, and has a lone pair. For $ZnAs_2$, on the other hand, the As is coordinated tetrahedrally to two Zn and two As atoms while the Zn bonds to four As atoms (29) utilizing the lone pair.

The addition of the group IV element results in the structure shown in Figure 2 for $CdGeAs_2$ (34). The bonding around the Cd remains unaltered but the lone pair of As in the binary compound is now utilized to form two covalent bonds with Ge making the As tetrahedrally bonded. In the $ZnM^{IV}As_2$, the bonding is the same as for $CdGeAs_2$. However, now the addition of the group IV element is effected by breaking the As-As bonds. The tetrahedral bonding structure results in a much more rigid structure than for materials such as the chalcogenides or amorphous As. The binary material structure is closer to that formed by the tetrahedrally coordinated group IV elements.

Four defect structures can arise from breaking the Cd-As and Ge-As bonds (Fig. 3). If the bonds are broken heterolytically with the electrons remaining on the more electronegative As atom, the structure shown in Figure 3(b) arises. The As has a lone pair which results in either a -1/2 or -1 charge depending on whether the As-Cd or As-Ge bond, respectively, is broken. The result is an ionic defect in which the electrons are paired; no electron spin signal is expected. Homolytic bond rupture (Figure 3(c)) results in charge formation from the Cd-As bond, but forms a neutral defect for the Ge-As bond. Both bond fragmentations, however, lead to unpaired electrons. Results of previous magnetic susceptibility experiments on glassy $CdGeAs_2$ (26) indicate that the density of such spin states is low (see Section II).

The bond defect pattern for the ternary compounds is analogous to that for the $A^{III}B^V$ compounds. For GeAs, it has been proposed that the defects are self-compensated by formation of homopolar bonds, i.e., Ge-Ge and As-As (32). A similar situation is possible for the ternary glasses as shown in Figure 3(d). Such compensation would reduce the spin density but may introduce new states in the gap because of the low energy of the homonuclear bonds. Additional theoretical work is necessary to quantify the energies associated with the defect formation in these ternary systems.

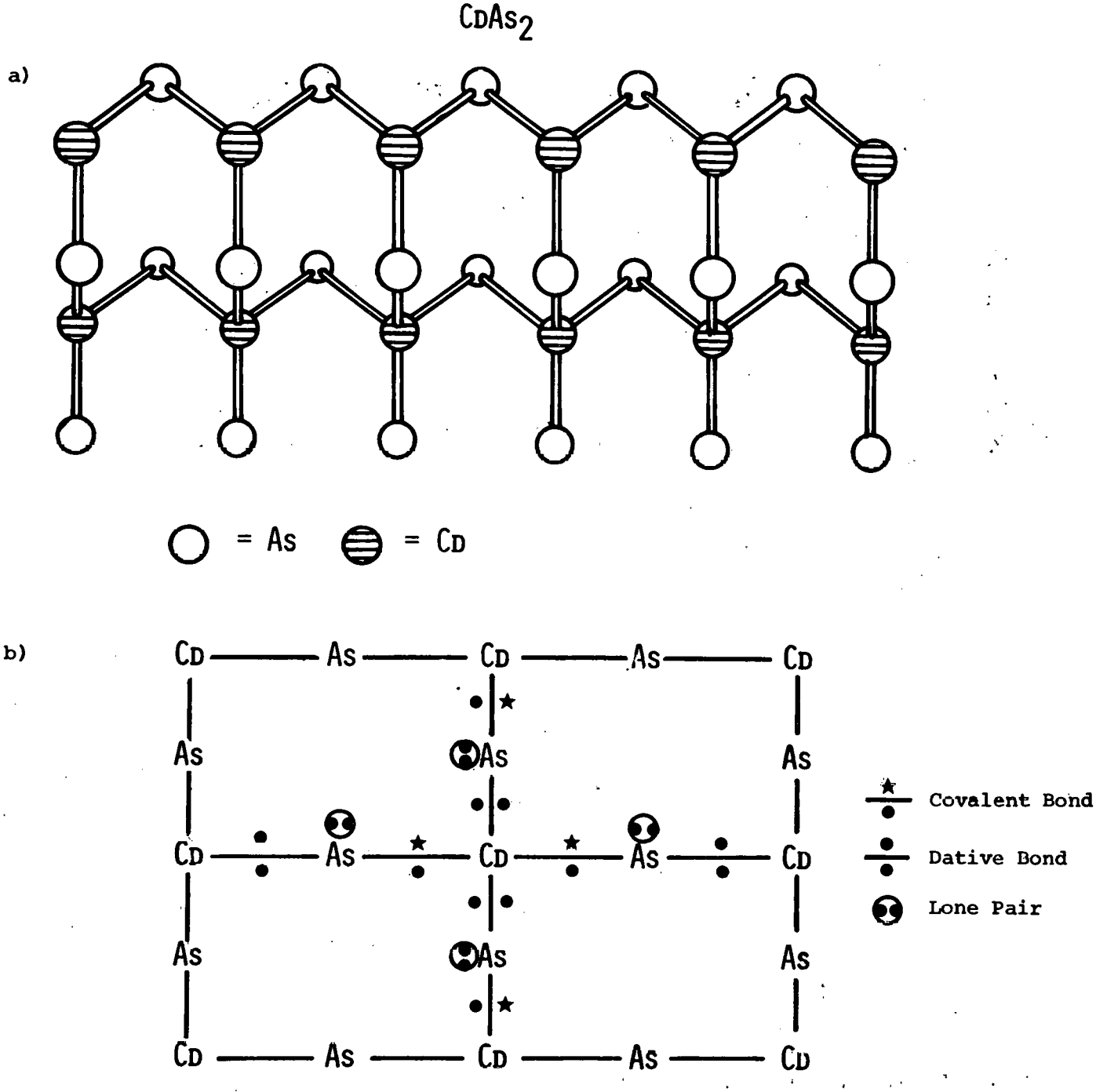

Fig. 1: Diagram of structure and bonding for $CdAs_2$. a) Perspective view showing the spacial orientation of the atoms. b) Schematic representation of the bonding.

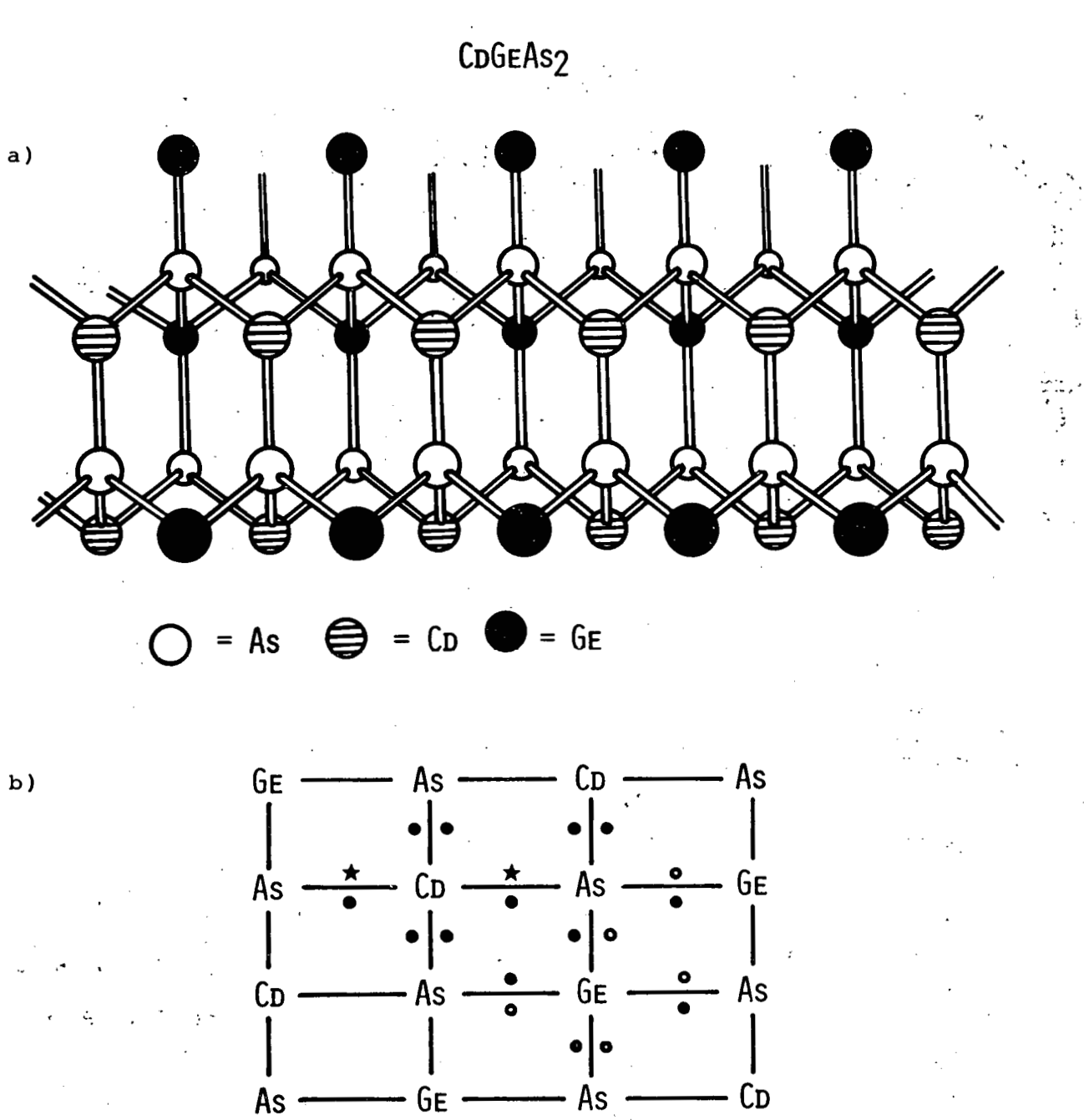

Fig. 2: Diagram of structure and bonding of ternary $A^{II}B^{IV}C_2^V$ compound $CdGeAs_2$. a) Perspective view showing the tetrahedral bonding of Ge within the $CdAs_2$ lattice. b) Schematic diagram of the bonding.

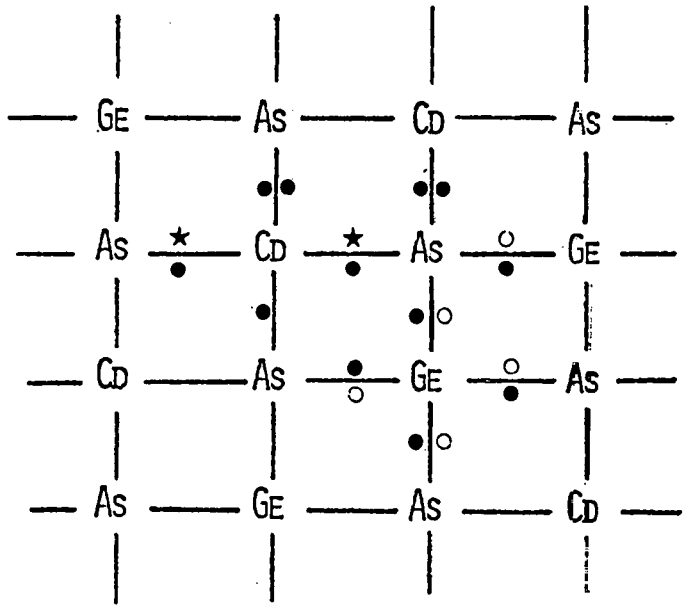

(a) Bonding of ternary system without defects.

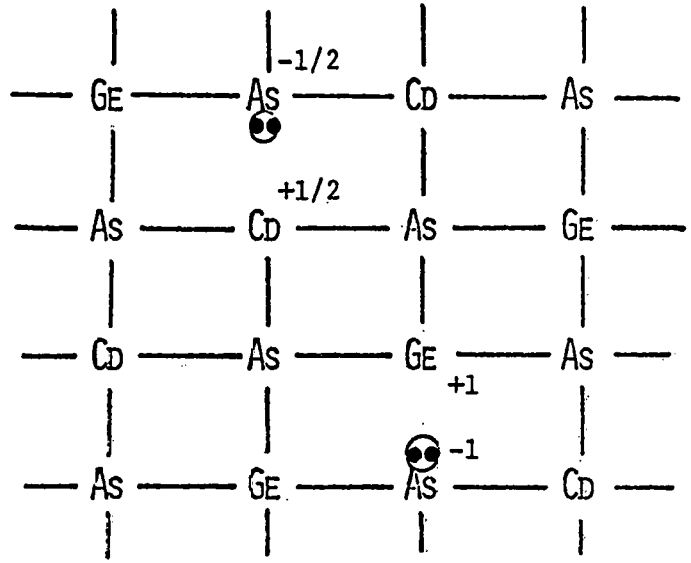

(b) Defect structure resulting from heterolytic Cd-As and Ge-As bond rupture.

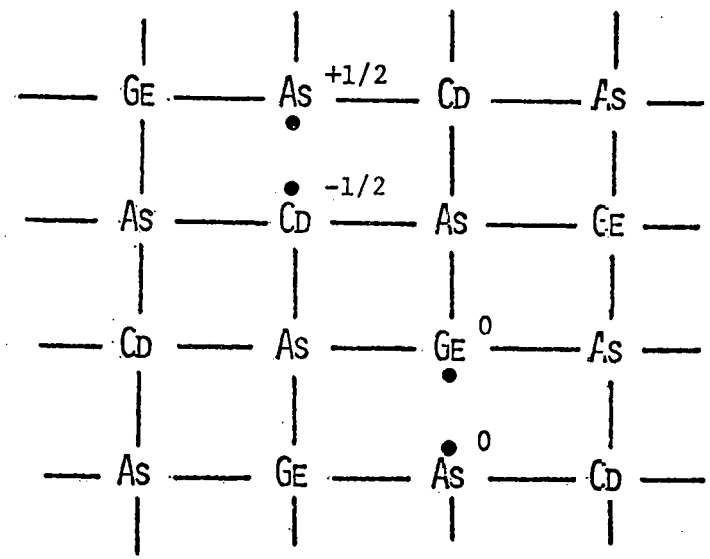

(c) Defect structure resulting from homolytic Cd-As and Ge-As bond rupture.

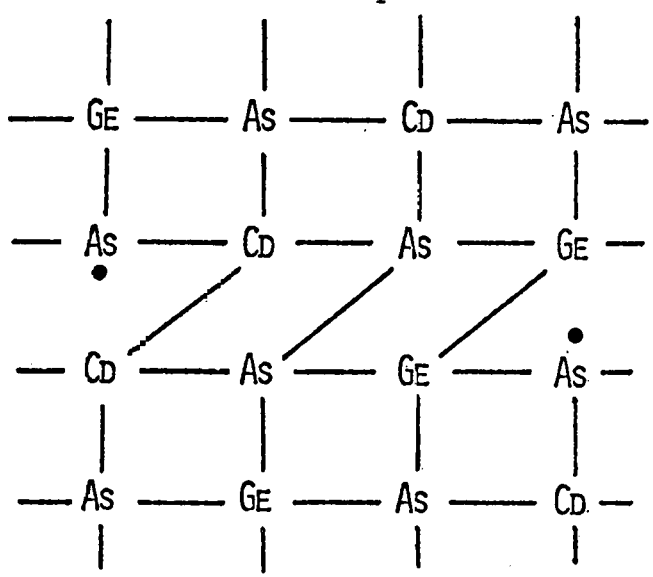

(d) Partial compensation of defect by formation of homonuclear bonds.

Fig. 3: Defect structures proposed for $CdGeAs_2$.

IV. SYNTHESIS OF BULK QUANTITIES OF $A^{II}B^{IV}C_2^V$ COMPOUNDS

None of the ternary chalcopyrite compounds of interest in this study were available commercially. The first attempts at preparation showed the need for developing careful preparative procedures for each compound. Many of the literature reports on the syntheses were too vague to be useful. All the ternary arsenides whose crystalline band gaps are in the useful region for solar energy photovoltaic application were successfully prepared in bulk quantities. The phosphides proved more difficult to make, and attempts at their synthesis were discontinued.

- Preparation of Ternary Arsenides. All the arsenides were prepared using the method described by Masuomoto (35) for $ZnSiAs_2$. In this procedure the constitutent elements (Cerac, 99.999% purity) were mixed in near stoichiometric amounts and sealed in an evacuated, thin-walled, quartz tube which had been coated with pyrolyzed graphite. The tube was placed in an oven and heated at a rate of 75°C/hr to a temperature less than 40°C above the melting point of the ternary product (see Table 2). Those mixtures with Sn were held at this temperature for only 3 hours before air cooling. The other samples were held at the elevated temperature overnight (≈15 hours) and then allowed to cool slowly in the oven. The samples yielded silver-gray ingots several millimeters in length (see Figure 4).

One sample of Cd, Ge, and As was heated to 800°C and held at that temperature overnight. The sample was removed from the oven and quenched in oil. The resulting material was a polycrystalline ingot of $CdGeAs_2$ rather than a glass. Apparently the relatively slow cooling that occurred between the time of removal of the sample from the oven and the quenching permitted crystallization. A smaller sample of Cd-Ge-As melted in a quartz tube without the graphite coating yielded an amorphous material when quenched in water.

- Preparation of Ternary Phosphides. Preparation of the ternary phosphides by simple fusion of the constituent elements was generally not possible. All attempts resulted in explosion or lack of reaction. The explosion was due to the pressure built up as the phosphorus vaporizes. At temperatures low enough to prevent explosion, the reaction did not occur.

An attempt was made to prepare $CdSnP_2$ by a two-step procedure using a single zone furnace. First, stoichiometric quantities of Cd, Sn, and red P were mixed in an evacuated, thin-walled quartz tube (i.d. 4 mm). The inside of the tube was not coated with graphite. The tube was brought to 500°C, maintained there for 20 hours, and then quenched

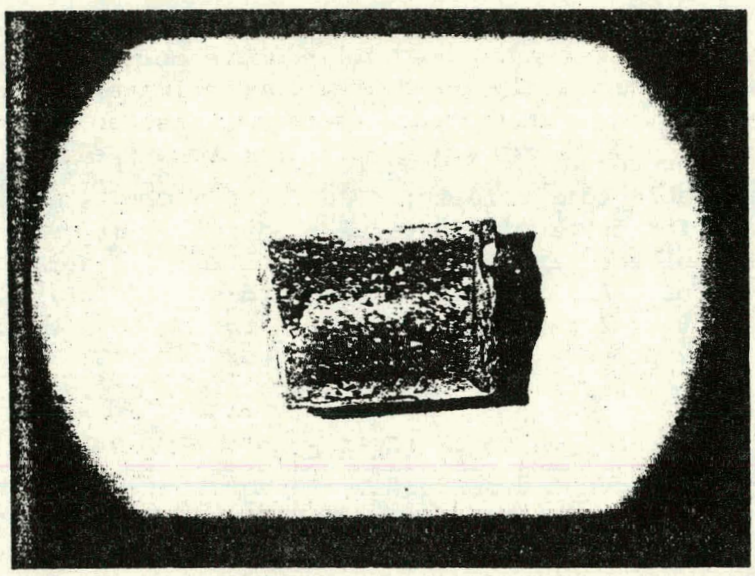

Magnification 8X

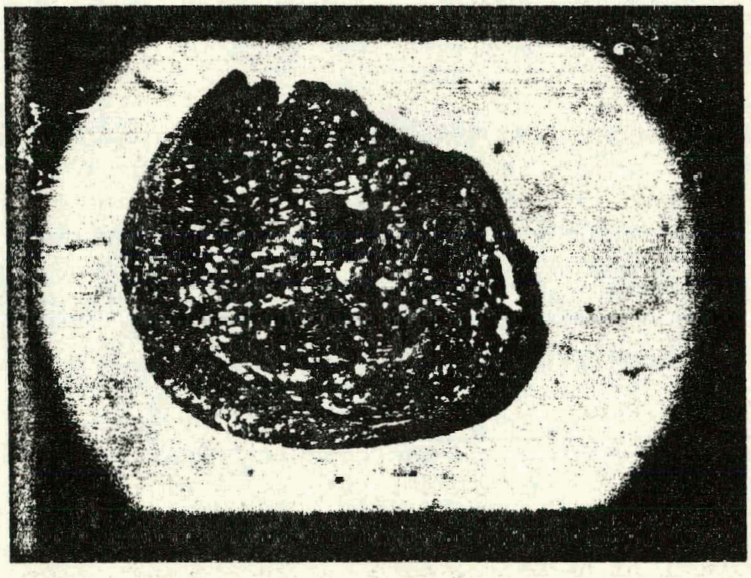

Magnification 16X

Fig. 4: $ZnSnAs_2$ polycrystalline ingot produced from fusion of stoichiometric amounts of the elements.

in cold water. The tube was then reheated to 650°C over a period of 6 hours and held at that temperature for 6 hours before rapid quenching. This procedure yielded a blood-red ingot approximately 15 mm long. While the x-ray spectra gave lattice parameters in reasonably good agreement with those in the literature for $CdSnP_2$, subsequent elemental analysis using atomic emission spectroscopy showed that the compound was Cd_3P_2.

An alternative method tried for producing the phosphides was melting the ZnP_2 or CdP_2 in the presence of the group IV element (36). The binary phosphides were prepared by the method of Rubenstein and Dean (37). The components were sealed in an evacuated quartz tube with the red phosphorus at one end and the metal (Zn or Cd) at the other. The tube was placed in a 3-zone furnace which was tilted about 20° to raise the phosphorus end. First the phosphorus end was heated to 350°C, and then the metal end was raised to a temperature slightly below the boiling point of the metal. The equilibrium temperature of the middle zone was about 500°C. After 12-36 hours the furnace was shut off, and the tube was allowed to cool slightly. Preparation of ZnP_2 in this manner resulted in a 50% yield. Approximately half of the material was formed as the monoclinic (black) modification. The remainder was the red, tetragonal form. CdP_2 was prepared in a similar manner, except that the tube was backfilled with nitrogen to a pressure of 1 atm. A small yield of the red tetragonal CdP_2 was obtained.

In order to increase the yield of CdP_2 production, the dissociation of Cd_3P_2 (Cerac, 99.5%) in an excess of phosphorus was attempted (38). The Cd_3P_2 was placed in one end of the tube and red phosphorus in the other. The phosphorus end was raised to 460-480°C and the Cd_3P_2 to 700°C. An orange-red ring of CdP_2 formed in the middle zone held at 600-640°C. While the yield was increased, it was still far below the 50% value obtained for ZnP_2 production.

• Analysis of Bulk Materials. The bulk polycrystalline material was analyzed by x-ray diffraction powder analyses and plasma emission spectroscopy. Table 4 compares the stoichiometric ratio of the elements in the starting mixture and the resulting ternary compound. It is seen that the composition of resulting ternary compounds is neither the exact stoichiometry for the pure compound nor the stoichiometry of the initial mixture. The discrepancy can be attributed to loss of the more volatile elements when sealing the quartz ampules under vacuum, incomplete reaction, and/or entrapment of unreacted material in the ingots which were not recrystallized.

The x-ray analysis data confirm the crystalline chalcopyrite state of the compounds. The lattice dimensions calculated from the diffraction angles are given in Table 4 along with the literature values. The differences between the literature and experimental values probably reflect the nonstoichiometric compositions of the ternaries and show the ease of introducing substitutional defects into these compounds.

TABLE 4

ELEMENTAL AND X-RAY ANALYSIS OF SYNTHESIZED TERNARY ARSENIDE COMPOUNDS

Compound	Stoichiometric Ratio[a]		Lattice Constants[b]					
			a(Å)		c(Å)		c/a	
	Starting[c] Material	Resulting[d] Ternary	This Work	Literature	This Work	Literature	This Work	Literature
$CdGeAs_2$	$CdGe_{0.9}As_{1.8}$	$CdGe_{0.6}As_{2.1}$	5.73	5.943	11.62	11.217	1.92	1.88
$CdSnAs_2$	$CdSn_{0.8}As_{1.8}$	$CdSn_{0.8}As_{1.5}$	6.05	6.093	11.73	11.92	1.93	1.96
$CdSiAs_2$	$CdSi_{1.2}As_{1.9}$	$CdSi_{1.2}As_{1.7}$	5.82	5.884	10.79	10.882	1.85	1.85
$ZnGeAs_2$	$ZnGe_{1.0}As_{2.1}$	$ZnGe_{0.3}As_{1.8}$	5.78	5.672	10.81	11.153	1.83	1.97
$ZnSnAs_2$	$ZnSn_{1.0}As_{2.2}$	$ZnSn_{1.0}As_{2.1}$	5.82	5.851	12.16	11.710	2.09	2.00
$ZnSiAs_2$	$ZnSi_{0.9}As_{1.9}$	$ZnSi_{1.7}As_{2.8}$	5.73	5.612	10.71	10.878	1.87	1.94

[a] Normalized to the Group II element.

[b] The precision of x-ray lattice parameters determined in this work is estimated as ± 0.10Å. The literature values are taken from the compilation in J. L. Shay and J. W. Wernick, Ternary Chalcopyrite Semiconductors: Growth, Electronic Properties, and Applications (New York: Pergamon Press, 1975), p. 7.

[c] Mole ratio of pure elements weighed into quartz tube before melting.

[d] Ratio of elements in polycrystalline ingots determined by plasma emission spectroscopy.

V. PRODUCTION OF TERNARY THIN FILMS BY EVAPORATION

Thin films offer one of the most promising methods of making solar cells using large scale production because of reduced material requirements and ease of covering large areas. Whereas considerable difficulties are encountered in making single crystal thin films, amorphous films are more easily obtained. The ternary $A^{II}B^{IV}C_2^V$ compounds which are the subject of the current research have exhibited a tendency to form glasses.

A computer search of the literature on $A^{II}B^{IV}C_2^V$ compounds revealed that thin films have been made by liquid phase epitaxy (LPE) (39,40), explosion in vacuum (41), and sputtering of polycrystalline materials (42). Since the goal of the LPE work was to produce orientated crystalline materials, it was not directly relevant to the fabrication of amorphous films.

Vacuum deposition seemed the most promising method for formation of amorphous thin films. $CdGeAs_2$, $ZnGeAs_2$ and $CdGeP_2$ have been formed by explosion in vacuum and $ZnGeAs_2$ by sputtering. The first method did not result in formation of films with the same stoichiometry as the bulk material; the films were deficient in Ge, the highest melting constituent of the compounds (41). Sputtering of $ZnGeAs_2$ onto an aluminum substrate, however, produced stoichiometric amorphous films (42). While poor stoichiometry was also reported for formation of $CdSiAs_2$ thin films by evaporation, better results were obtained by sputtering (5). Use of chemical vapor deposition techniques as reported for production of thin films of $ZnSiAs_2$ (3) were not deemed suitable for making amorphous films because the high temperatures involved exceed the glass transition temperature leading to polycrystalline material.

These results indicated that vacuum evaporation of the ternary compounds would probably lead to nonstoichiometric films. The best results should obtain for the higher melting ternaries such as $ZnSiAs_2$ because the vapor pressures of the compound and the high melting group IV element are comparable. Poor stoichiometries were found, however, for all the thin films produced from bulk ternary $A^{II}B^{IV}C_2^V$ compounds. Much better results were obtained using the binary compounds of zinc and arsenic, $ZnAs_2$ and Zn_3As_2. Amorphous thin films of Zn_3As_2 have been prepared previously by vacuum evaporation on glass substrates at 20°C (31).

A. Amorphous Film Formation by Vacuum Evaporation - Apparatus and Procedure

An Edwards automatic evaporator, Model 12EA, was used for the vacuum deposition. The unit consists of a 12" bell jar with a 4" oil (D.C. 704) diffusion pump which pumps down to 2×10^{-5} torr in about an

hour. Ultimate vacuum with the present Peltier thermoelectric cooled baffle is 6×10^{-7} torr after eight hours of continuous pumping. The system is fitted with a low voltage, high current power supply for resistive heating of boats and filaments. Several different sample holders have been tried including tungsten shallow dimple boats, filament heated alumina crucibles and deep tantalum baskets. The latter have been most successful in producing films with minimal loss of material from jumping out of the boat. It also provides the most directed vapor transport towards the substrate.

A quartz lamp heater can be used to heat the substrate at any time during the deposition. For the initial films, there was no monitoring of the source or substrate temperature. Later a chromel-alumel thermocouple attached to the source or substrate monitored the temperature. In the last two months of the contract period, an argon glow discharge system (plasmatron) was installed to allow ion cleaning of the substrate, in vacuo, before the deposition.

The general procedure for evaporation was as follows: A small amount of finely ground sample was placed in the heating element. The substrate was a pyrex slide or aluminum stub which had been cleaned in an ultrasonic bath of ethanol, rinsed with acetone, and dried in air. The height of the substrate above the sample could be varied between 3" (low) and 5" (high). The slide was protected during the initial heating stages by a metal shutter. After mounting the sample and substrate, the system was evaucated to less than 10^{-5} torr. The substrate was cleaned for 15 minutes with the argon plasma. Current was passed through the refractory boat. When the desired temperature and pressure were reached, the shutter was opened and the material allowed to coat the bottom of the slide.

B. Production of Thin Films of Ternary Arsenides

• $CdSnAs_2$. Two films were prepared from $CdSnAs_2$, using a tungsten boat. The same sample was used for both films. For the first film, the system was evacuated to a pressure of 4×10^{-6} torr and the current brought to 45A over a 5 minute period. The shutter was opened and the film allowed to form for 3 hours. The second film was formed by rapidly bringing the current to 50A when the pressure reached 5×10^{-6} torr. The evaporation continued at this current for 6 hours.

• $CdSiAs_2$. Three films were prepared from a single sample of $CdSiAs_2$, using an Al_2O_3 crucible. For the first film, the current was brought to 10 amps over a 10 minute period with the pressure at 8×10^{-6} torr. The shutter was opened and evaporation proceeded for 1 hour. A second film was formed by immediately raising the current to 35A. After 5 minutes at this current, the shutter was opened and evaporation took place for 30 minutes at a pressure of 6×10^{-6} torr. The third film was deposited at a pressure of 1.5×10^{-5} torr. The current was brought to 45A over 15 minutes. The shutter was opened and current increased to 50A

over the next 30 minutes. Evaporation continued for 45 minutes; however, only a small area of film formed on the substrate. It is presumed that the slide itself became too hot to allow the film to form, since the interior of the bell jar was well coated. A fourth film of $CdSiAs_2$ was prepared from a fresh sample of starting material. For this film, the substrate was raised to the higher position, about 5" above the source. The sample was contained in an Al_2O_3 crucible. The current was raised quickly in 2-3 minutes to 45A. As soon as the pressure reached 1.0×10^{-5} torr, the shutter was opened and evaporation proceeded for 2 hours.

• $ZnSiAs_2$. A single film of $ZnSiAs_2$ was prepared. The homogeneity of the starting material was suspect even though the atomic emission results show relatively good stoichiometry. It was only partially reacted during its synthesis from the starting elements because the ampoule was not held at the high temperature for a long enough time period. To prepare the film, the sample was contained in an Al_2O_3 crucible with the substrate held 5" above the source. The current was raised over 5 minutes, and the shutter was opened. Evaporation proceeded for 2 hours.

• Results. The films produced from all the materials had a metallic mirror finish which generally adhered well to the substrate. They were insoluble in simple inorganic acids. There was no sign of deterioration of the material when stored in air, although some of the films did begin to peel off the glass substrate. Observation of the films prepared with a metallograph at 20X magnification showed many pits and striations in the film.

Plasma atomic emission was used to determine the elemental compositions of the films and estimate their thickness. The samples were prepared by dissolving the film in hot aqua regia and diluting with 1% HCl. A SMI Spectraspan IV spectrometer, utilizing a D.C. argon plasma, was used to measure the solution concentrations. This instrument is fully microprocessed and reads directly in concentration. The ratios of the concentrations yields the stoichiometry of the sample. The approximate film thicknesses were calculated from the weight of the dissolved material, using an average density of 5 gm/cm^3. The results are shown in Table 5.

• Discussion. Most of the necessary data for evaluating a priori the best set of conditions, i.e., vapor pressure, decomposition temperature, etc., were unavailable for the compounds. Some of the compounds either melt peritectically or decompose below their melting point. The resulting film will be deficient in the low vapor pressure (i.e., group IV) element. Our initial attempts at vacuum deposition of the ternary compounds, therefore, were primarily of a trial and error nature to delineate the problems. The composition of the evaporated films for the compounds listed in Table 5 is decidedly different from the starting material. The results are consistent with what is known about the thermal decomposition of the compounds.

Because of the difficulty in obtaining stoichiometric ternary films, attempts were made to make films from the binary arsenic compounds $CdAs_2$

TABLE 5

ELEMENTAL COMPOSITION AND THICKNESS OF TERNARY ARSENIDE FILMS PREPARED BY EVAPORATION

Starting Compound	Composition of Film	Calculated Film Thickness (μm)[a]
$Cd_{1.0}Sn_{0.8}As_{1.5}$	$Cd_{1.0}Sn_{2.8}As_{8.3}$	0.04
	$Cd_{0}Sn_{2.8}As_{0.43}$[b]	0.07
$Cd_{1.0}Si_{1.2}As_{1.8}$	$Cd_{1.0}Si_{0.1}As_{0.3}$	0.2
	$Cd_{1.0}Si_{0.1}As_{1.8}$	0.3
	$Cd_{1.0}Si_{1.0}As_{1.3}$	insufficient material
	$Cd_{1.0}Si_{0.3}As_{0.4}$	0.05
$Zn_{1.0}Si_{0.3}As_{1.8}$[c]	$Zn_{1.0}Si_{0.1}As_{0.1}$	0.11

[a] Calculated from atomic emission concentration data assuming density of 5g/cc.

[b] Only a trace of cadmium was detected.

[c] The sample may not have had a homogeneous stoichiometry.

and $ZnAs_2$. Little success was obtained with $CdAs_2$, a result similar to that reported by Burton and Slack (5). In contrast, the initial studies with $ZnAs_2$ showed better stoichiometries of the films and a more detailed investigation of this system was undertaken.

C. $ZnAs_x$ Thin Film Preparation

A number of $ZnAs_x$ films were made from polycrystalline $ZnAs_2$ which was obtained from Cerac with a stated purity of 99.99%. The substrates were pyrex slides mounted three inches above a deep tantalum basket containing the $ZnAs_2$. The basket gave a more directionalized vapor than the small tungsten dimple boats.

The system was evacuated to less than 5×10^{-6} torr before the deposition began. In general, the basket was first heated by passing a current of 100A through the basket for 1-2 minutes until the sample has "degassed" and the pressure dropped below 1×10^{-5} torr. During this initial heating a shutter was placed between the source and substrate. The shutter was then opened and the deposition began. The deposition was controlled by manually adjusting the current delivered to the basket and monitoring the temperature of either the basket or substrate. The evaporation conditions for a number of films are given in Table 6. The last column of the table shows that films were prepared with a wide range of stoichiometries. Different heating programs were attempted to control the stoichiometry.

The effect of substrate temperature on the composition of the film is evident from Table 6B. The temperature was monitored by attaching a thermocouple to the top of the substrate with high temperature cement. Without any additional heating, the substrate temperature rose to about 50°C due to the heat from the evaporation source. This temperature resulted in films with both the best stoichiometries and surface properties. When the substrate was heated to about 110°C with a quartz radiant heater, the resulting film developed a spider web-like pattern. Magnified metallographic photographs of such a surface is shown in Figure 5. This deterioration of the film occurred both when deposition was made at a constant temperature of 110°C and when the substrate temperature was raised from 60°C to 110°C during the deposition. Above 110°C, the deterioration of the film seemed to cease. Depositions on substrates held at much higher temperatures, >170°C, did not show any crazing but the films were found to be very deficient in arsenic.

The results of the two pairs of films made from the same $ZnAs_2$ sample in the tantalum basket show that the material remaining in the basket after a deposition is deficient in arsenic. A direct measurement of the residue in the basket confirmed the low percentage of arsenic. There is little doubt, therefore, that decomposition of the $ZnAs_2$ occurred in the basket (30), probably to give Zn_3As_2 and As_4, and the latter sublimed away because of its higher vapor pressure. Further decomposition

TABLE 6

EXPERIMENTAL CONDITIONS FOR PRODUCTION OF THIN FILMS BY EVAPORATION OF CRYSTALLINE $ZnAs_2$

Film No.	Substrate or Basket (Temp °C)	Maximum Current (A)	Deposition Pressure (Torr x 10^6)	Deposition Time (min)	Elemental Composition[a]
A. Temperature Not Monitored					
070479A[b]	-	55	12.5	30	$ZnAs_{2.0}$
072479A[b]	-	52	8	60	$ZnAs_{0.7}$
072579A[b]	-	45	50	36	$ZnAs_{1.4}$
B. Substrate Temperature Monitored during Deposition					
080679A	47	135	2	4	$ZnAs_{2.1}$
080779A[c]	46	150	7	4	$ZnAs_{0.4}$
091079	49	145	3	5	$ZnAs_{1.5}$
082179A	51	127	4	5	$ZnAs_{2.3}$
082379A[c]	59	145	10	5	$ZnAs_{0.3}$
080379A	60	140	0.8	25	$ZnAs_{1.0}$
082879A	108	135	8	7	$ZnAs_{1.5}$
083179A	179	145	20	3	$ZnAs_{0.2}$
082979A	221	145	40	2	$ZnAs_{0.1}$
C. Tantalum Basket Temperature Monitored during Deposition					
102579A	325	140	2	7	$ZnAs_{1.7}$
102979B	390	140	200	5.8	$ZnAs_{0.5}$
100579B	390	160	800	4.8	$ZnAs_{1.6}$
100579A	395	150	3	1.5	$ZnAs_{2.1}$
112779A	395	140	700	9.5	$ZnAs_{1.4}$
110279AA	397	135	50	5.6	$ZnAs_{0.1}$
101179A	397	135	30	0.5	$ZnAs_{2.2}$
100479B	400	150	3	1.0	$ZnAs_{3.8}$
110179A	400	135	15.5	4.3	$ZnAs_{0.7}$
102979A	410	140	4	6	$ZnAs_{0.6}$
092679A	411	135	6	15	$ZnAs_{1.8}$
092079B	424	140	40	10	$ZnAs_{2.6}$
092479B	425	145	0.3	12	$ZnAs_{0.5}$
092579B	440	135	20	14	$ZnAs_{1.2}$
092079A	490	140	40	13	$ZnAs_{1.0}$
091779A	500	145	30	3	$ZnAs_{3.0}$
100479A	580	150	3	2.2	$ZnAs_{0.9}$

[a]
[b]Determined by plasma emission.
[c]Tungsten boat used for depositions.
Film prepared using same $ZnAs_2$ starting material as previous film.

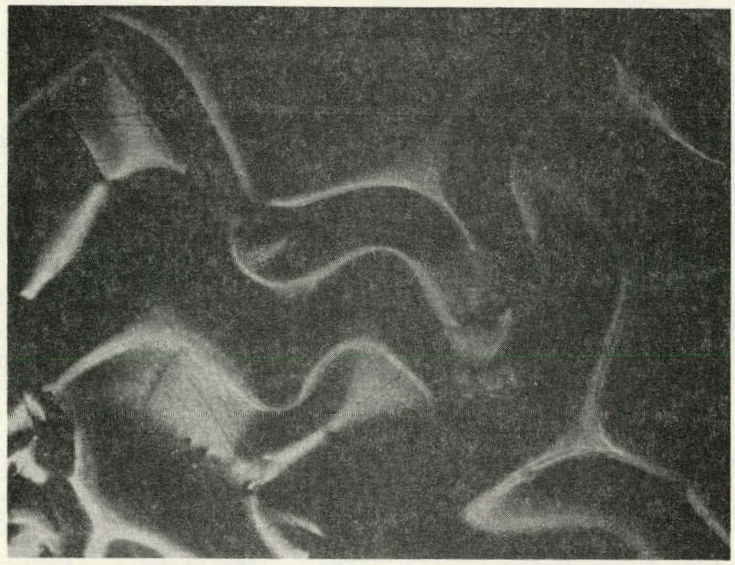

(a) 800X Magnification - Unpolarized Light.

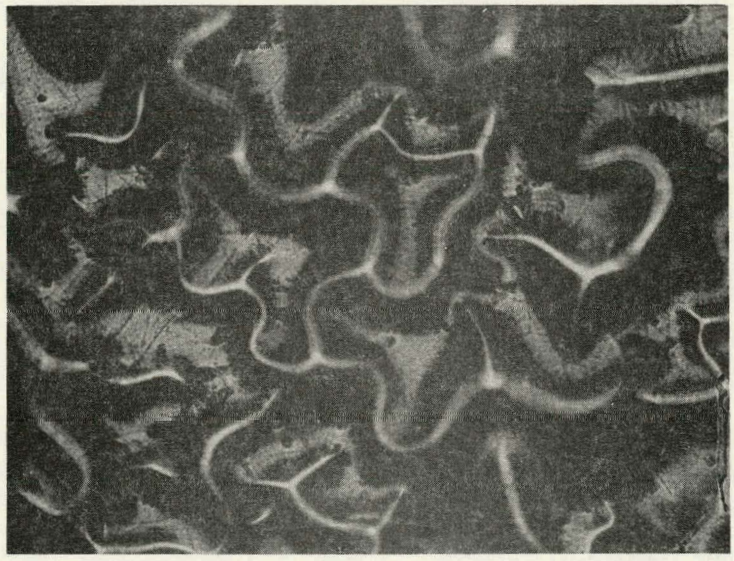

(b) 200X Magnification - Polarized Light.

Fig. 5: Metallograph photographs of Sample No. 082879A ($ZnAs_{1.5}$) showing cracking and pitting of surface.

of Zn_3As_2 to Zn and As_4 cannot be ruled out. Despite these complications several of the films had stoichiometries in the range expected between Zn_3As_2 ($ZnAs_{0.7}$) and $ZnAs_2$.

In an attempt to improve the control of the film stoichiometry, the thermocouple was attached directly to the tantalum basket. The opening of the basket was also covered with a thin layer of quartz wool to prevent splattering of material onto the substrate. After the degassing, the current was quickly raised to about 135-140A and deposition begun. The current was cut off as the temperature neared 360°C. When the temperature dropped below 200°C, the current was raised again to 140A. This cycle of raising and lowering temperature was repeated for several minutes. Any time the temperature exceeded 395°C, the shutter was momentarily closed. Deposition occurred less evenly and at a much slower rate than in previous techniques. Deposited films were usually shiny and dark, although some films had silvery-white areas. It had been reported that significant decomposition in a closed system did not occur until 400°C (43). In our case under vacuum conditions, however, significant decomposition has occurred judging from the stoichiometries of the films listed in Table 6C. Indeed, there seemed to be little correlation of film stoichiometry with deposition time, maximum temperature of the basket, or pressure during deposition. The two films listed in Table 6C with very high arsenic concentrations were made with the shutter open during the initial degassing step supporting the belief that As_4 is a major volatile component during the initial warm-up. Similar results have been reported recently in attempts to make stoichiometric films of $CdAs_2$ by thermal evaporation (5).

Additional experiments of $ZnAs_x$ film production showed that the stoichiometry was improved if the quartz wool was removed and if the heating rate was increased. It is now possible to make films routinely with bulk stoichiometries in the range of Zn_3As_2 to $ZnAs_{2.1}$ but control within this range is very difficult.

VI. CHARACTERIZATION OF AMOPRHOUS $ZnAs_x$ FILMS

A. Physical and Chemical Properties

The films deposited on unheated substrates were dark with a metallic finish. The thickness ranged from 0.1 to 1.2 μm. In general, they adhered well to the substrate and did not appear to degrade by exposure to the atmosphere. SEM micrographs of one of the films is shown in Figure 6. At high magnification (>500X), the films show some pitting and furrows in the surface. There was no indication of crystallization. X-ray analysis of several of the films confirmed that they were amorphous.

The bulk analysis by plasma emission did not provide any information on the homogeneity of the film. The films did not dissolve in simple inorganic acids indicating the absence of metallic islands of Zn which might have arisen from phase separation. The EDAX analysis showed the film to be chemically homogeneous in the plane of the slide. Similarly, the Auger results showed no Zn or As islands on the surface within the 3 μm resolution of the measurements. Depth profile studies on two of the films indicated some change in stoichiometry with depth as might be expected for deposition from a sample undergoing decomposition. EDAX spectra on film 091079A (Figure 7) were taken at the thick and thin portion of the film. The thicker portion showed a higher ratio of Zn.

Auger analysis was performed on Sample No. 100579B ($ZnAs_{1.6}$) to provide a depth profile of the composition of the film. A polycrystalline sample of $ZnAs_2$, as received from Cerac, Inc. was analyzed to provide a reference spectrum. The change in the zinc to arsenic ratio as a function of sputtering time is shown in Figure 8; ru and rs are the ratios of the unknown and standard, respectively, and R is the ratio of ru to rs. Near the surface of the film there was a large excess of zinc. After 30 seconds of sputtering, this excess was reduced and a constant ratio was obtained in the remainder of the film that is removed by ion milling.

The concentration of zinc in atomic percent was calculated using the equation

$$C_{Zn} = \frac{ru/1.68}{[ru/1.68] + 1}$$

where 1.68 was the sensitivity factor of $ZnAs_2$. After 60 seconds of sputtering, the zinc atomic percent was 40% using the equation. This corresponded to a stoichiometry of $ZnAs_{1.5}$ which was in good agreement with the bulk stoichiometry of the film as measured by atomic emission.

a)

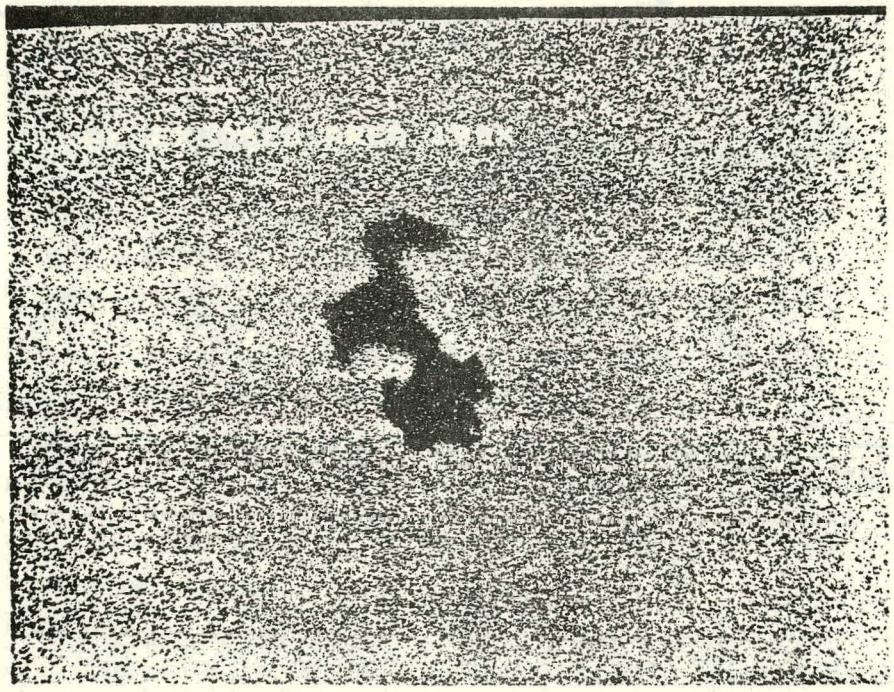

b)

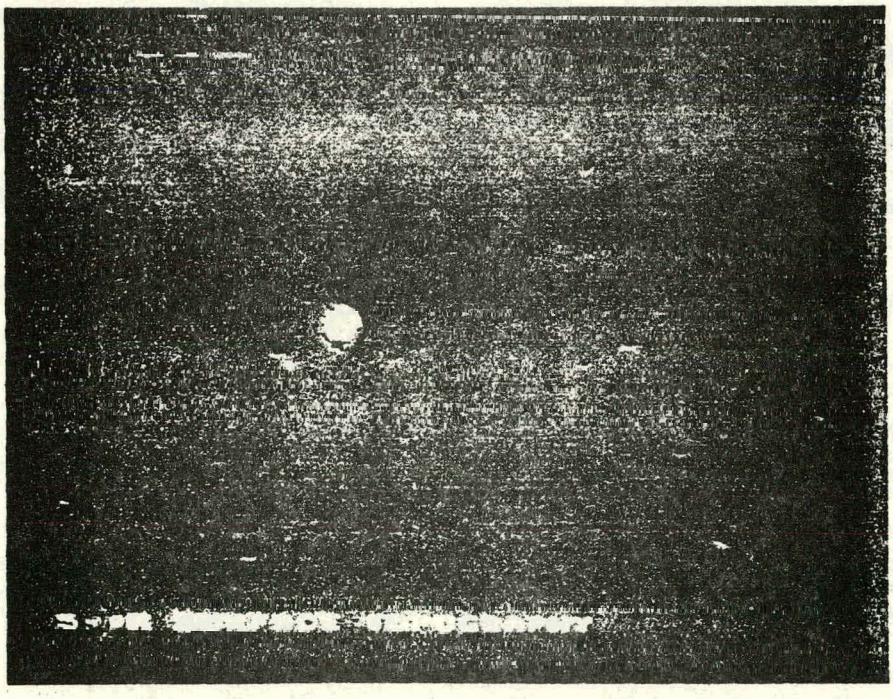

Fig. 6: SEM micrographs of $ZnAs_{1.5}$ film Sample No. 091079A. a) 100X magnification showing thin portion of film with Al substrate showing through. b) 500X magnification showing some pits and bumps on the surface. (SEM done by Photometrics, Inc.)

a)

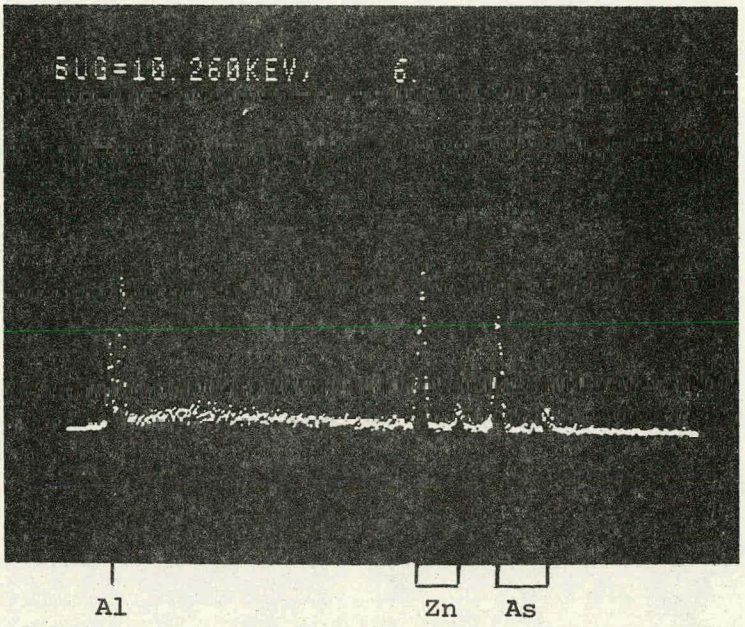

b)

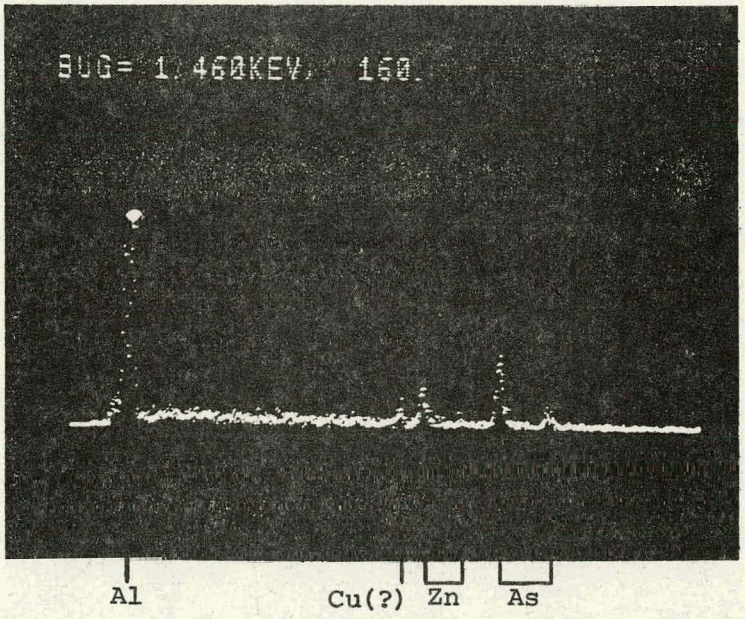

Fig. 7: EDAX spectra of $ZnAs_x$ film Sample No. 091079A. a) Spectrum from homogeneous area of film showing Zn and As in the ratio of about 4:3. b) Spectrum from the thin area in film (see Fig. 2a) showing more intense Al peak and ratio of Zn to As of about 1:2 as expected for $ZnAs_2$ stoichiometry. (Spectra taken by Photometrics, Inc.)

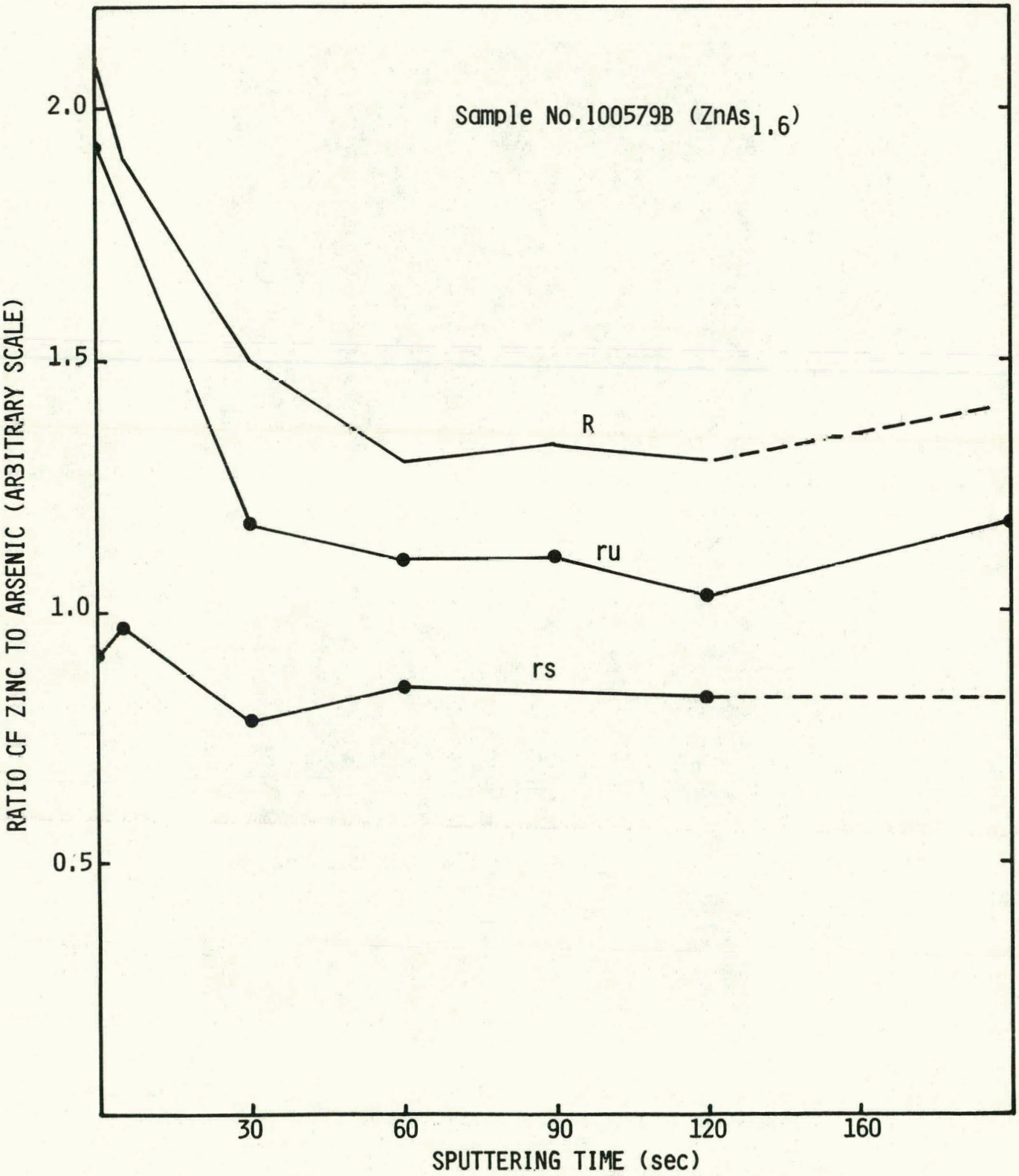

Fig. 8: Ratio of zinc to arsenic intensity of Auger lines plotted against time of ion milling. rs is ratio for $ZnAs_2$ standard, ru the ratio for the unknown and R the ratio of ru to rs. (Spectra done by Photometrics, Inc.)

Additional Auger measurements at several other places on the film indicated it was homogeneous in the plane of the film.

The conclusion from these results is that homogeneous films are produced by the evaporation technique and that the measurement of the bulk stoichiometry is a good indication of the microscopic composition.

B. Film Thickness

The thickness of the films was determined in three ways, two of which require assumptions in the calculations. The first method merely involved calculation of thickness from the measured concentrations observed in the atomic emission studies. The weight of the compound dissolved divided by the area of the dissolved sample gave the value of weight/cm^2. If this value was divided by the density, the thickness of the film was obtained. The density, of course, depended on the type of material as well as how densely it was deposited on the substrate. Since this information was not known for the present amorphous materials, a value of 5 gm/cm^3 was used in the calculations. For comparison, crystalline As has a density 5.6 gm/cm^3, c-Zn_3As_2-5.5 gm/cm^3 and c-$ZnAs_2$-5.12 gm/cm^3. Amorphous arsenic has a density of 4.3-5.3 gm/cm^3 and other amorphous materials such as Si and Ge have densities less than their crystalline forms. In addition, if the films were even less dense than the amorphous bulk material, the thicknesses would be greater than calculated. The assumed density, therefore, was probably a maximum value and gave a minimum thickness for the films.

The second calculation of thickness was based on the interference patterns observed in the absorption spectra. Maxima and minima were observed either on the plateau of the absorption or on the baseline before the absorption edge. Since it could not be determined where the interference pattern began, the formula was used for successive maxima or minima, namely (44),

$$t = \frac{i\,\lambda_o\lambda_i}{2n(\lambda_o-\lambda_i)\cos\phi'}$$

where t was the thickness, λ_o and λ_i the wavelengths of two maxima or minima, i the number of complete cycles from λ_o to λ_i, n the refractive index of the film and ϕ' the angle of refraction. ϕ' was assumed equal to 0° since the light of the spectrometer impinged perpendicular to the plane of the slide. A value of 4.1 is used for n for the amorphous films based on the results reported in Ref. 31.

The third method used a Dektak surface profiler. Since this instrument measured the thicknesses directly, the results are considered the most reliable. Table 7 summarizes the thickness obtained by each method. In general, the Dektak values were bracketed by the lower atomic emission values and higher values from the interference pattern calculation. The two indirect methods, however, gave an order of magnitude estimate of the thickness for use when Dektak measurements could not be made.

TABLE 7

COMPARISON OF THICKNESS OF $ZnAs_x$ FILMS IN μm MEASURED BY DIFFERENT TECHNIQUES

Sample No.	Composition	Dektak	Atomic Emission[a]	Interference Pattern[b]
110179A	$Zn_3As_2(ZnAs_{0.7})$	0.28	0.11	0.46
102879A	$Zn_3As_2(ZnAs_{0.6})$	0.32	0.09	0.47
102979AN	$Zn_3As_2(ZnAs_{0.9})$	0.28	-	-
112779A	$ZnAs_{1.4}$	0.32	0.15	-
102579A	$ZnAs_{1.7}$	0.17	0.16	0.55
100479B	$ZnAs_{3.8}$	0.17[c]	0.75	0.95

[a]Calculated assuming a density of 5.0 g/cm^3.
[b]Assuming a refractive index of 4.1.
[c]Thickness is a lower limit since it was measured at edge of film away from center of deposition source.

C. Thermal Stability

To obtain information about the thermal stability of the amorphous $ZnAs_x$ films, two films were evaporated on 4" x 4" pyrex plates. The measured stoichiometries were $ZnAs_{1.4}$ and $ZnA_{0.5}$. The films were scraped off the plates and analyzed by differential scanning calorimetry from 25° to 377°C under atmospheric conditions by Cambridge Analytical Services. The heating rate was 80°C/min. After the DSC, an X-ray analysis of the sample was performed.

No peaks attributable to a phase change were observed for either sample. Since the scan rate was relatively fast, transitions occurring at temperatures above 325°C would probably not be observed. The X-ray analysis of the heated samples, however, showed no pattern attributable to crystallization. To check these results, portions of the film still on the plates were annealed at 375°C for 1 hour in the atmosphere. No obvious physical changes occurred as a result of the heat treatment. X-ray analysis of the annealed samples was inconclusive. The X-ray diffraction showed no obvious crystalline peaks, however, the characteristic amorphous spectrum was also absent. The measured stoichiometry of the samples changed, however, from $ZnAs_{1.4}$ to $ZnAs_{2.2}$ and from $ZnAs_{0.5}$ to $ZnAs_{0.6}$. The $ZnAs_{2.2}$ sample also had an absorption spectra giving an optical band gap of about 1.0 eV, much closer to that reported for crystalline $ZnAs_2$ than the amorphous material value of 1.5 eV (see Section VI.D).

In another study, Sample No. 102979A ($ZnAs_{0.6}$) was annealed *in vacuo* at 100°C for 4 hours. A quartz radiant heater was used as the

heat source. Again the film showed no physical changes after this period. Atomic emission spectroscopy, however, showed a decrease in zinc concentration and a weight loss of about 30%. The stoichiometry of the annealed film was $ZnAs_{0.9}$. Annealing at this lower temperature resulted in no appreciable change in the absorption spectra.

No definite conclusions can be drawn about the temperature limits for annealing $ZnAs_x$ films. Annealing does seem to improve the stoichiometry of the films. Post-annealing at temperatures ≥100°C does not introduce the problems observed with crazing of the films when depositing them on substrates at 110°C.

D. Optical Absorption Spectra

The absorption of the films was measured using a Cary 14 Spectrometer. An uncoated slide was used in the reference side of the instrument; background measurements with two blank slides showed no absorption. The observed absorption of a thin film was the result of three factors: absorption by the material, reflection from the surfaces of the film and substrate, and scattering of the light. Only the first factor was important in determining the absorption coefficient α of a film. While the scattering could be neglected, for the highly reflective films of $ZnAs_x$, the reflection term made a substantial contribution to the observed absorption.

To calculate the α values, the method of Freeman and Paul was used (45). This treatment was strictly valid only in the short wavelength region, where the absorption was large.

To calculate α,

$$\alpha = -\frac{1}{d} \ln \left\{ \frac{1}{B} \left[A + \left(A^2 + 2BT \left\{ 1 - R_2 R_3 \right\} \right)^{\frac{1}{2}} \right] \right\}$$

where:

$A = -(1-R_1)(1-R_2)(1-R_3)$

$B = 2T(R_1R_2 + R_1R_3 - 2R_1R_2R_3)$

$R_1 = \left[\frac{n-1}{n+1}\right]^2 \quad R_2 = \left[\frac{n-n_o}{n+n_o}\right]^2 \quad R_3 = \left[\frac{n_o-1}{n_o+1}\right]^2$

n = refractive index of film

n_o = refractive index of substrate; 2.23 for pyrex

T = observed transmission

d = film thickness

The refractive index of $ZnAs_x$ films, $0.6 \geq x \geq 0.9$ was taken from the values observed by Zdanowicz and Pawlikowski (31) for Zn_3As_2. For $ZnAs_x$, $1.4 \geq x > 2.0$, the refractive index used was 4.1.

The adjusted optical spectra are shown in Figure 9 and plots of $(\alpha h\nu)^{\frac{1}{2}}$ vs. $(h\nu)$ in Figure 10. The shape of the optical spectra of the films is in good agreement with that obtained for other amorphous materials.

The absorption spectra of the films fall into three categories. The three samples with stoichiometry near Zn_3As_2 all show comparable absorption spectra and have a band gap of 1.15-1.25 eV. This range is in good agreement with the value of 1.14 eV reported in the literature (31) and is about 0.2 eV larger than that for crystalline Zn_3As_2 (46). A second set of curves arise for films with stoichiometries of $ZnAs_{1.7}$ and $ZnAs_{2.1}$. These films absorb at wavelengths of higher energy indicating a band gap of about 1.5 eV. This value, therefore, is assigned to amorphous $ZnAs_2$ for which no previous information is available. The absorption spectra for films with stoichiometries intermediate between the two stable compound forms lies to the red side of amorphous Zn_3As_2. This result can be explained by assuming that the film is composed of a mixture of Zn_3As_2 and As_4, the latter having a band gap of about 1.0 eV (47). Films produced with As/Zn stoichiometries greater than 3.5 also gave absorption spectra with band gaps on the order of 1 eV.

E. Electrical Properties

The resistivity of the a-$ZnAs_x$ films was measured using the four-point probe technique in a square geometry. The apparatus is shown in Figure 11. A ECO Model 551 Potentiostat/Galvanostat was used to supply constant current. Resulting voltages were read from a Hewlett-Packard Model 3645A High Impedance Digital Multimeter.

Since the films were much thinner than the probe spacings, the resistivity was found using the equation (44)

$$\rho = \frac{2\pi t}{\ell n 2} \frac{V}{I}$$

The variables are defined by:

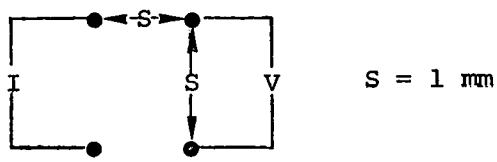

and t is the thickness of the film. To alleviate the problem of contact between the film and the probes, Al was evaporated onto the film. This

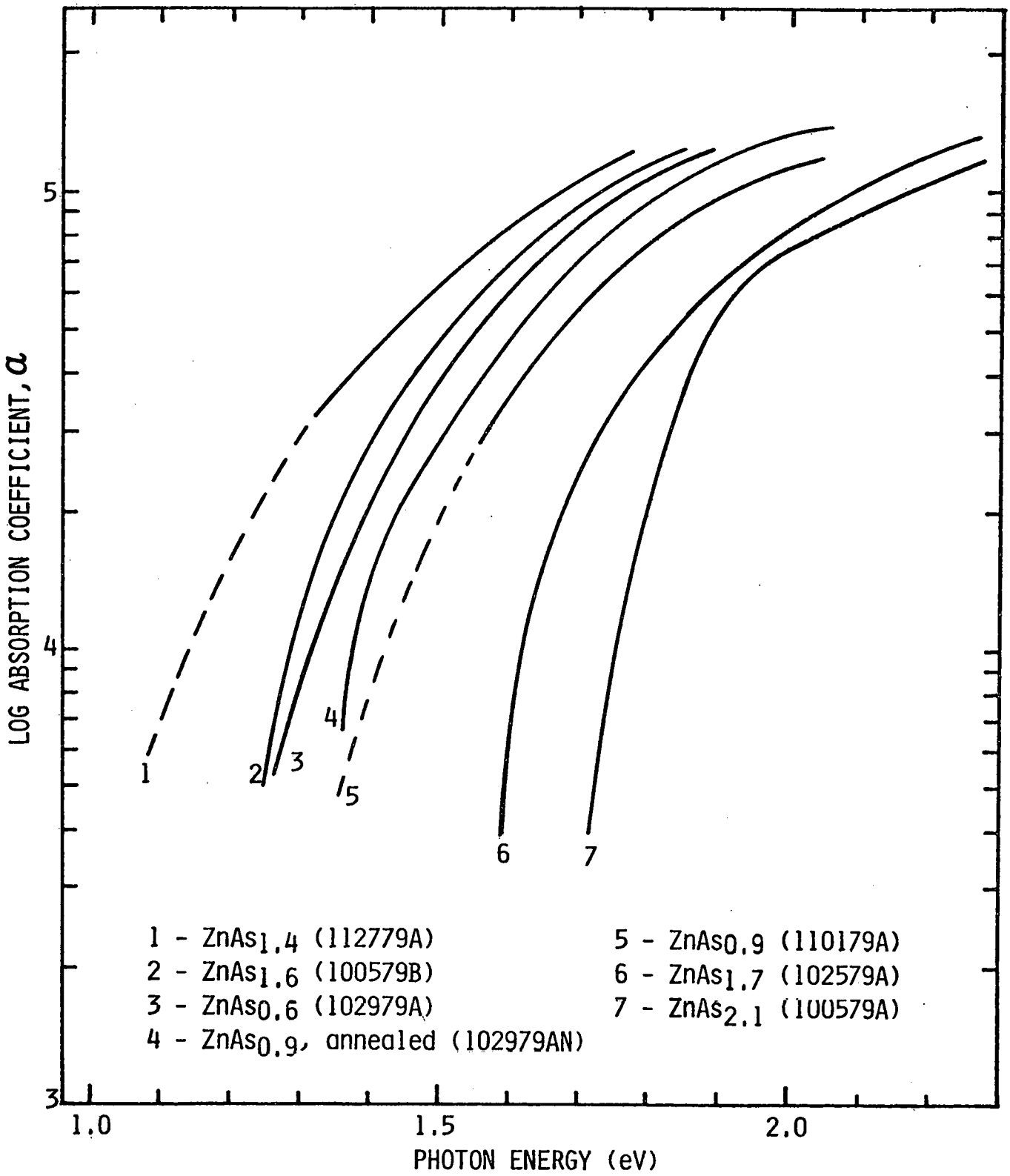

Fig. 9: Absorption coefficient for several $ZnAs_x$ films.

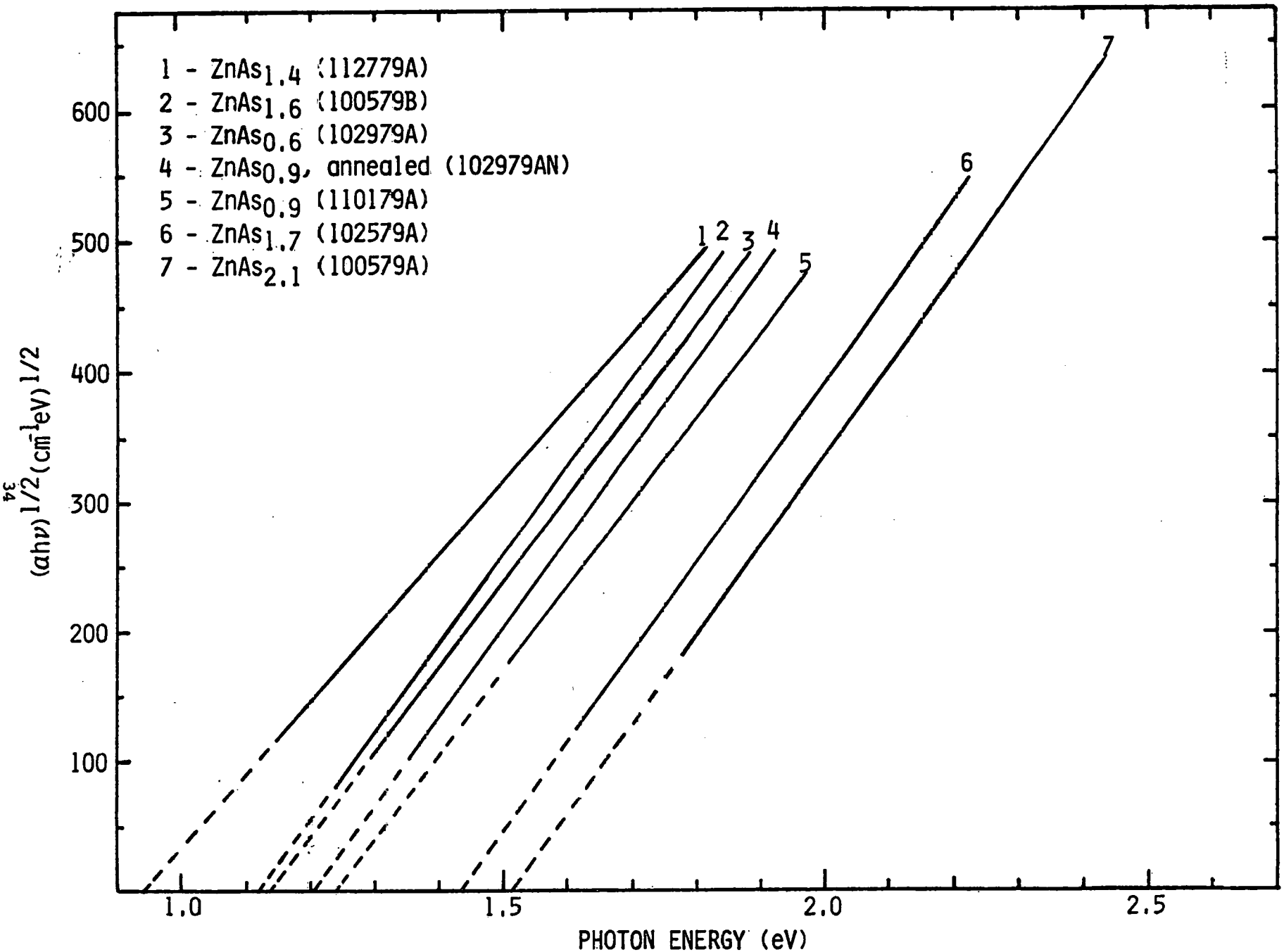

Fig. 10: Optical absorption edge of $ZnAs_x$ films.

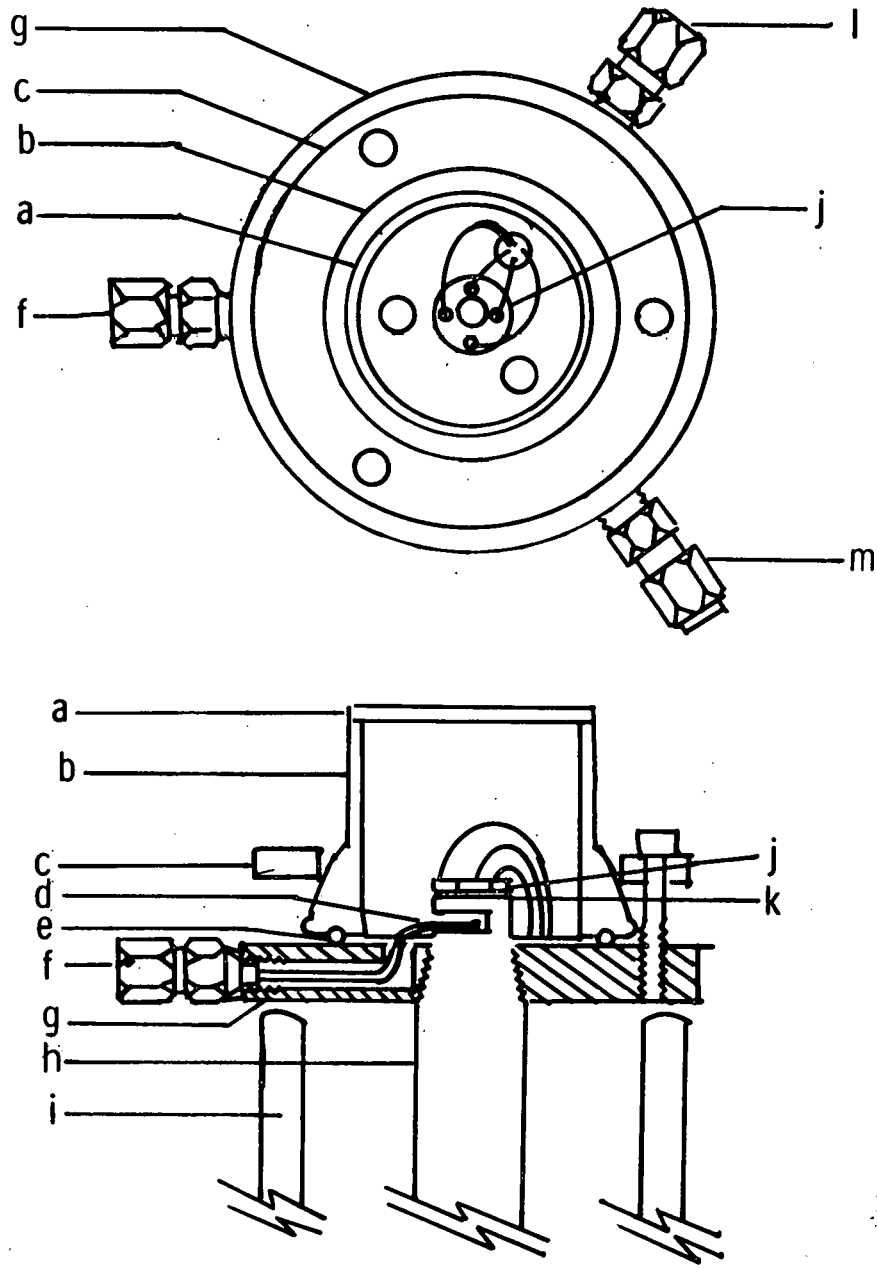

Fig. 11: Apparatus for resistivity measurements. a) Pyrex window epoxied to joint; b) glass 40 mm O-ring joint; c) aluminum hold-down ring; d) thermocouple; e) Viton O-ring; f) Conax 2-lead vacuum fitting; g) Teflon base; h) copper bar; i) Dewar flask; j) mica washer with four-point probe leads; k) sample film; l) Conax 4-lead vacuum fitting; m) pumping port with Swagelok fitting.

was accomplished by first masking the slide with an aluminum plate. The plate had four, 1 mm holes spaced about 1 mm apart. Deposition was accomplished by heating the Al slowly to about 120A in a tungsten boat until the Al melted and wet the boat. The current was lowered and then immediately raised to 160A. The shutter was opened for 1-2 seconds to allow deposition. This procedure resulted in an even Al layer on the unmasked areas. Comparison of two and four probe measurements showed Al formed an ohmic contact with the films.

The resistance of the films was measured as a function of temperature over the range from 25° to 100°C. Measurements at subambient temperatures were not possible because of loss of contact between the probes and the film. The room temperature resistivities are given in Table 8 using the thickness values measured with the Dektak.

TABLE 8

OPTOELECTRICAL PROPERTIES OF $ZnAs_x$ FILMS

Sample No.	Stoichiometry	Resistivity[a] (Ω-cm)	Activation Energy (eV)	Photoconductance[a,b] (Ω-1)
102579A	$ZnAs_{1.7}$	1.7×10^2	0.54	1.6×10^{-10}
102979A	Zn_3As_2	1.3×10^3	0.47	3.0×10^{-9}
110179A	Zn_3As_2	1.1×10^3	0.11	-

[a] Room temperature.
[b] Illuminated with Xenon arc lamp with a pyrex filter at an intensity of 40 mW/cm^2.

The conductance was plotted on a logarithmic scale as a function of the reciprocal of absolute temperature in Figure 12 for two films. The curves could be divided into a low temperature and high temperature region. At lower temperatures, the conductance increased slowly until about 60°C where the increase became more rapid. In order to rule out that instrumental effects were responsible for the double-sloped curve, the system was checked using a polycrystalline, doped Fe_2O_3 pellet. The oxide had a room temperature resistivity of 1.8×10^6Ω-cm. No discontinuity occurred over the temperature range from 0°-100°C. Linear behavior with a single slope was observed.

The conductance data for zinc arsenide can be explained by a two mechanism conduction model proposed by Mott and Cohen, Fritzsche and Ovshinsky (48). Low temperature conduction occurs by excitation of carriers into the band tail (hopping). At higher temperatures, conduction

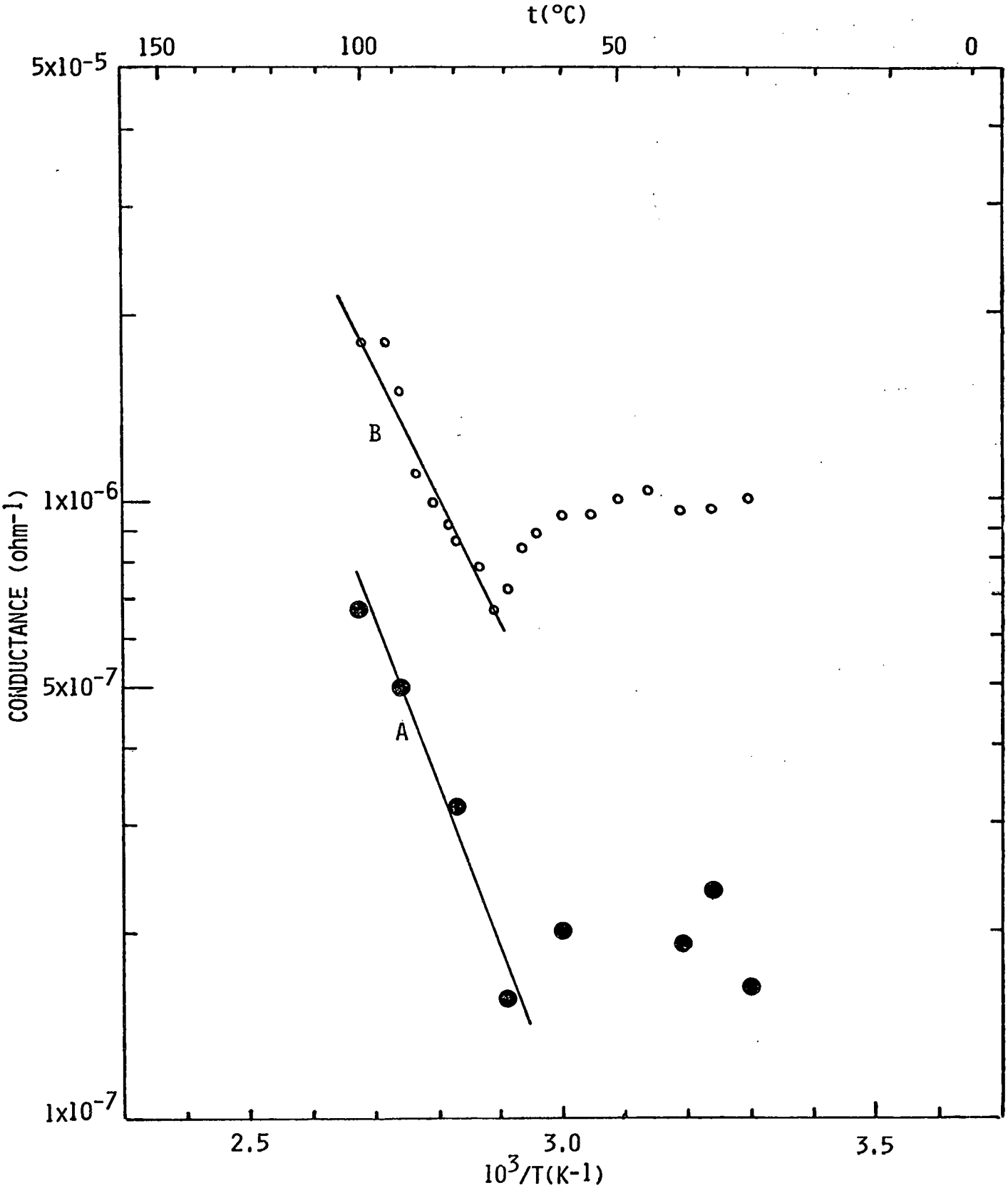

Fig. 12: Temperature variation of d.c. conductance for $ZnAs_x$ films.
A = 102979A, $ZnAs_{0.6}$, E_a = 0.55 eV
B = 102579A, $ZnAs_{1.7}$, E_a = 0.43 eV

occurs by excitation of carriers into the conduction band. The conductivity equations for both mechanisms are of the same form so both show linear behavior for a log σ vs. 1/T plot. The activation energy for hopping, however, is much less than that for conduction into the band. The activation energy for conduction in the band tail is generally between 0.1 and 0.3 eV. Our data is in good agreement with these values. The activation energy for the high temperature region should be about half the optical band gap. In many chalcopyrite systems, however, the value is smaller due to strong carrier compensation (1). Occurrence of the two-step mechanism could be determined from the effect of temperature on the thermopower. If, and only if, one mechanism was operating the slope of log of thermopower vs. 1/T would be the same as observed for the conductivity data.

Type Measurement. A measurement of the conductivity type was made on film 102979A ($ZnAs_{0.6}$) using the rectification technique and a three-probe configuration (44). Application of the ac signal resulted in a positive voltage indicating that the film was p-type. Crystalline Zn_3As_2 was also reported to be p-type (Table 3).

F. Photoconductivity

The photoconductivity of two $ZnAs_x$ films was measured. Large aluminum contacts separated by 1 mm were evaporated onto the films. Silver wires were silver epoxied onto the contacts. The change in current on applying a bias voltage was measured in the dark and illuminated by a Xenon lamp with a pyrex filter. The I-V curves at two different light intensities is shown in Figure 13 for amorphous zinc arsenide films with stoichiometries of (a) $ZnAs_{0.6}$ and (b) $ZnAs_{1.7}$. The photoconductivity values are given in Table 8.

The wavelength dependence of the photoconductivity for the two films was measured at λ = 905, 765 and 650 nm. The photocurrent, PC, normalized to the absorbed light intensity was calculated using the equation (49):

$$PC = \frac{\Delta i}{AF}$$

where Δi is the measured photocurrent, A the illuminated area and F the absorbed photon flux. F was calculated from the absorption spectra in Figure 9 and the reflection coefficients for Zn_3As_2 films (31). Incident light intensities were about 50 $\mu W/cm^2$. If the quantum efficiencies, η, for formation of a carrier from each absorbed photon is assumed to be one, the photoconductive gain, G, is equal to PC/e where e is the charge on the electron. The values for two different films are listed in Table 9. For the Zn_3As_2 film there is little change in the gain over the wavelength region as expected, since all the energies are considerably above the band gap. For the $Zn_3As_{1.7}$ film, there is an inverse relationship with increasing photon energy. The explanation for this trend is not clear.

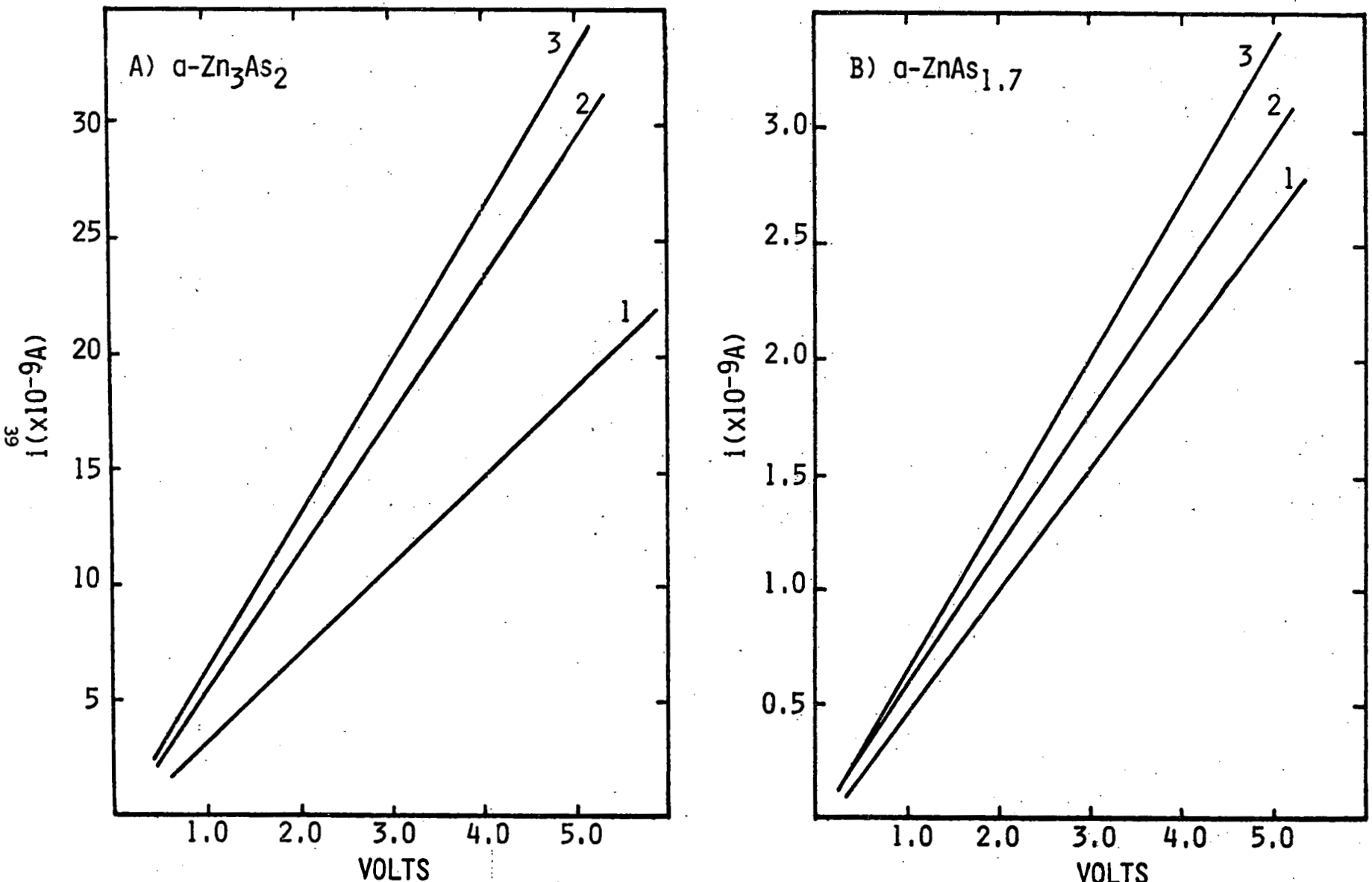

Fig. 13: i-V plots for dark and illuminated films of amorphous $ZnAs_x$ at two light intensities from filtered Xenon lamp. 1 = dark; 2 = 10 mW/cm^2; 3 = 40 mW/cm^2.

TABLE 9

SPECTRAL DEPENDENCE OF PHOTOCONDUCTIVITY
OF $ZnAs_{0.6}$ FILM

Wavelength (nm)	Energy (eV)	Δi[a] (amperes)	F (photons/cm^2-sec)	G[b]	$\mu\tau$ (cm^2/V)
a-$ZnAs_2$					
950	1.37	13.6×10^{-9}	7.7×10^{13}	3.3×10^{-3}	7.4×10^{-6}
765	1.62	8.0×10^{-9}	4.9×10^{13}	3.1×10^{-3}	6.9×10^{-6}
650	1.91	4.5×10^{-9}	9.4×10^{13}	1.4×10^{-3}	3.1×10^{-6}
a-$ZnAs_{1.7}$					
765	1.62	2.5×10^{-10}	0.8×10^{13}	5.9×10^{-4}	1.7×10^{-6}
650	1.91	3.5×10^{-10}	6.0×10^{13}	1.1×10^{-4}	3.2×10^{-7}

[a] Measured at bias voltage of 5.0V for Zn_3As_2 and 3.5V for $ZnAs_2$. Area = 0.66 cm^2.

[b] Assuming the quantum efficiency of carrier generation is one.

Measurements of the gain value as a function of intensity at 650 nm, however, revealed that it decreased with increasing number of photons absorbed.

If the assumption of unit quantum efficiency is correct, the mobility lifetime product, $\mu\tau$, is equal to GL^2/V where L is the distance between the contacts and V is the bias potential. The experimental values are included in Table 9.

VII. SUMMARY AND RECOMMENDATIONS

The work performed during the contract period on the ternary $A^{II}B^{IV}C_2^V$ chalcopyrite systems proved them very difficult to form in stoichiometric thin films by simple evaporation processes. Near stoichiometric films could be made, however, from evaporation of crystalline $ZnAs_2$. Depending on the conditions used either amorphous $ZnAs_2$ or Zn_3As_2 films were deposited. The two materials had optical band gaps of 1.5 and 1.2 eV, respectively. The absorption spectrum provides a diagnostic for the stoichiometric purity of the films.

The as-deposited films are p-type and stable in air. Resistivities are on the order of $10^3\Omega$-cm. Both Zn_3As_2 and $ZnAs_2$ films exhibit photoconductivity. While the response is much smaller than for amorphous silicon, no attempt has yet been made to optimize the response by annealing or chemical modification of the material.

The results obtained thus far indicate that amorphous zinc arsenide offers considerable potential for development as a solar cell material. Both zinc and arsenic are abundant and inexpensive materials. The band gap and strong absorption coefficient make the material ideal for utilization of the solar spectrum. Finally, zinc arsenide is photoconductive in the as prepared films, although a great deal of work needs to be done to improve the film quality.

It is premature to address the questions of maximum efficiency, minimum degradation and large scale production for an emerging amorphous material such as zinc arsenide. Production by thermal evaporation must be evaluated relative to other methods of formation such as sputtering. The film's quality must be improved by thermal annealing and chemical passivation of the defects leading to a more resistive material and higher photoconductivity. Doping experiments should then be initiated to produce p- and n-type materials with improved transport characteristics. Simple heterojunction and Schottky cells can then be fabricated and tested for diode quality and photovoltaic properties. These areas are the tasks defined for the continuing work on the $ZnAs_x$ films.

VIII. REFERENCES

1. J. L. Shay and J. H. Wernick, Ternary Chalcopyrite Semiconductors: Growth, Electronic Properties and Applications (New York: Pergamon Press, 1975).

2. V. D. Prochukhan and Yu.V. Rud, Fiz. Takh. Poluprovodn., 12, 209 (1978).

3. J. E. Andrews, Quarterly Technical Progress Reports Nos. 1 and 2, under DOE Contract DE-AC04-79ET23001, Research Triangle Institute, April-September, 1979.

4. M. A. Littlejohn, "Study of II-IV-V_2 Compound Semiconductors for Solar Cell Applications," Proceedings of Photovoltaics Advanced Materials Review Meeting, October 24-26, 1978, Vail, Colorado, p. 505.

5. L. C. Burton and L. H. Slack, Quarterly Technical Progress Reports Nos. 1-3, under DOE Contract DOE/ET/23007, Virginia Polytechnic Institute and State University, April-December, 1979.

6. K. W. Mitchell, Photovoltaics Advanced R&D Annual Review Meeting, Sponsored by Solar Energy Research Institute, Denver, Colorado, September 17-19, 1979, p. 387.

7. V. N. Brudnyi, D. L. Budnitskii, M. A. Krivov, R. V. Masagutova, V. D. Prochukan and Yu.V. Rud, Phys. Stat. Sol. A, 50, 379 (1978); V. N. Brudnyi et al., ibid., 49, 761 (1978); V. N. Brudnyi et al., ibid., 35, 425 (1976).

8. B. R. Pamplin and R. S. Feigelson, Mat. Res. Bull., 14, 263 (1979).

9. G. W. Isler, H. Kildal and N. Menyk, J. Electron. Mat., 7, 737 (1978).

10. E. Ziegler, W. Siegel, G. Kühnel and E. Buhrig, Phys. Stat. Sol. A, 48, K63 (1978).

11. K. Winkler, U. Schulz and K. Hein, Krist. Teck., 13. 137 (1978).

12. A. Horak, I. Mitotkowski and J. Weszka, ibid., 13, K65 (1978).

13. J. C. Rife, R. N. Dexter, P. M. Bridenbaugh and B. W. Veal, Phys. Rev. B, 16, 4491 (1977).

14. A. S. Broshchevskii, N. A. Goryunova, F. P. Kesamanly and D. W. Nasledov, Phys. Stat. Sol., 21, 9 (1967).

15. N. A. Goryunova, Proceedings of Ninth International Conference on Physics of Semiconductors (Leningrad: Nauka, 1978), Vol. 2, p. 1198.

16. H. Fritzsche in Amorphous and Liquid Semiconductors, J. Tauc, ed. (New York: Plenum Press, 1974).

17. D. R. Uhlmann, J. Non-Cryst. Solids, 7, 337 (1972).

18. D. D. Thornburg, Thin Solid Films, 45, 95 (1977).

19. J. P. DeNeufville and H. K. Rockstad, Proceedings of Fifth International Conference on Amorphous and Liquid Semiconductors (London: Taylor and Francis, 1974), p. 419.

20. L. Cervinka, A. Hruby, M. Matyas, T. Simecek, J. Skacha, L. Stourac, J. Tauc and V. Vorlicek, J. Non-Cryst. Solids, 4, 258 (1970).

21. J. Tauc, L. Stourac, V. Vorlicek and M. Zavetova, Proceedings of Ninth International Conference on Physics of Semiconductors (Leningrad: Nauka, 1978), Vol. 2, p. 1251.

22. R. Callaerts, M. Denayer, F. H. Hashmi and P. Nagels, Discuss. Faraday Soc., 50, 27 (1970).

23. a) T. Satow, O. Uemura and S. Watanabe, Phys. Stat. Sol. A, 44, 731 (1977); b) O. Uemura and T. Satow, ibid., 44, 303 (1977).

24. N. Van Dong, T. H. Danh, B. Auguin and A. Defresne, ibid., 33, 295 (1976).

25. M. Matyas, J. Non-Cryst. Solids, 8-10, 592 (1972).

26. F. J. DiSalvo, B. G. Bagley, J. Tauc and J. V. Waszczak, Proceedings of Fifth International Conference on Amorphous and Liquid Semiconductors (London: Taylor and Francis, 1974), p. 1043.

27. M. Popescu, R. Manaila and R. Grigorovici, J. Non-Cryst. Solids, 23, 229 (1977).

28. A. Catalano, J. V. Masi and M. Convers Wyeth, Technical Report No. 1 EC/PV/TR/79/3, Institute of Energy Conversion, May 1979.

29. M. E. Fleet, Acta Cryst., B30, 122 (1974).

30. Z. A. Munir, M. E. Benavides and D. J. Meschi, High Temp. Sci., 6, 73 (1974) and references therein.

31. W. Zdanowicz and J. M. Pawlikowski, Acta Phys. Polon., A38, 11 (1970).

32. S. Ovshinsky and D. Adler, Contemp. Phys., 19, 109 (1978).

33. M. Kastner, D. Adler and H. Fritzsche, Phys. Rev. Letters, 37, 1504 (1976).

34. L. Cervinka, R. Hosemann and W. Vogel, J. Non-Cryst. Solids, 3, 294 (1970).

35. K. Masumoto, S. Isomura and W. Goto, J. Phys. Chem. Solids, 27, 1939 (1966).

36. S. A. Mughal, A. J. Payne and B. Ray, J. Mat. Sci., 4, 895 (1969); B. Ray, A. J. Payne and G. J. Burrell, Phys. Stat. Sol., 35, 197 (1969).

37. M. Rubenstein and P. J. Dean, J. Appl. Phys., 41, 1777 (1970).

38. W. Zdanowicz and A. Wajakowski, Phys. Stat. Sol., 10, K93 (1965).

39. S. M. Bedair and M. A. Littlejohn, J. Electrochem. Soc., 125, 952 (1978) and references therein.

40. A. Horak, I. Miotkowski and J. Weszka, Krist. Tech., 13, K65 (1978).

41. V. G. Baryshev, N. S. Boltivets, A. S. Borshchevskii, N. A. Goryunova and P. T. Oreshkin. Sov. Phys. Semicon., 4, 308 (1970).

42. W. Braun and M. Cardona, Phys. Stat. Sol. B, 76, 251 (1976).

43. An.N. Nesmeyanov, B. Z. Iofa and A. A. Strel'nikov, Zhur. Fiz. Khim., 32, 955 (1958).

44. W. R. Runyan, Semiconductor Measurements and Instrumentation (New York: McGraw-Hill Company, 1975).

45. E. C. Freeman and W. Paul, Phys. Rev. B, 18, 4288 (1978).

46. J. Misiewicz and J. M. Pawlikowski, Solid State Commun., 32, 687 (1979).

47. G. N. Greaves, S. R. Elliot and E. A. Davis, Adv. Phys., 28, 49 (1979).

48. W. F. Mott and E. A. Davis, Electronic Processes in Non-Crystalline Materials (Clarendon Press, Oxford Press, 1979).

49. D. A. Yates, C. M. Penchina and J. E. Davey in Amorphous and Liquid Semiconductors, J. Stuka and W. Brenig, eds. (London: Taylor & Francis, 1974), Vol. 2, p. 617.

☆ U.S. GOVERNMENT PRINTING OFFICE: 1981-740-145/2723